(2)

Space Applications Corporation
System Engineering Technologies, Inc.
University of Washington

SBIR Phase I Final Report:

Unconventional Signal Processing Using the Cone Kernel Time-Frequency Representation

by

John Carothers
Space Applications Corporation
Seattle Operations
6632 S. 191st Place, Suite E-103
Kent , WA 98032

and

Ernest W. Swenson
System Engineering Technologies,Inc.
P.O. Box 845
Edmends, WA 98020

30 October 1992

DISCLAIMER NOTICE

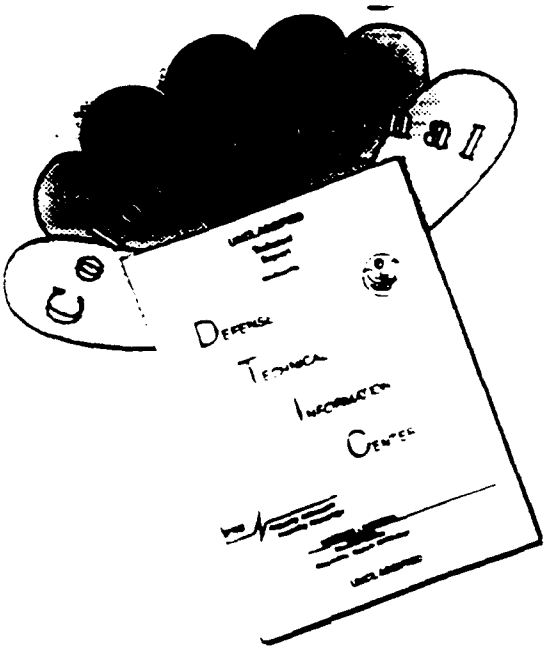

THIS DOCUMENT IS BEST QUALITY AVAILABLE. THE COPY FURNISHED TO DTIC CONTAINED A SIGNIFICANT NUMBER OF COLOR PAGES WHICH DO NOT REPRODUCE LEGIBLY ON BLACK AND WHITE MICROFICHE.

REPORT DOCUMENTATION PAGE

Form Approved
OMB No. 0704-0188

1. AGENCY USE ONLY (Leave blank)	2. REPORT DATE	3. REPORT TYPE AND DATES COVERED
	30 October 1992	Final Report: 4/1/92 to 10/31/92

4. TITLE AND SUBTITLE

SBIR Phase I Final Report:
Unconventional Signal Processing Using the Cone Kernel Time-Frequency Representation

5. FUNDING NUMBERS

Contract:
N00014-92-C-0096

6. AUTHOR(S)

J. Carothers and E.W. Swenson*

7. PERFORMING ORGANIZATION NAME(S) AND ADDRESS(ES)

Space Applications Corporation
Seattle Operations
6632 S. 191st Place, Suite E-103
Kent, WA 98032

8. PERFORMING ORGANIZATION REPORT NUMBER

9. SPONSORING/MONITORING AGENCY NAME(S) AND ADDRESS(ES)

Office of Naval Research
Department of the Navy
800 N. Quincy Street, Code: 1512B:EAM
Arlington , VA 22217-5000

10. SPONSORING/MONITORING AGENCY REPORT NUMBER

N/A

11. SUPPLEMENTARY NOTES

* System Engineering Technologies, Inc,, P.O. Box 845, Edmonds, WA 98020

12a. DISTRIBUTION/AVAILABILITY STATEMENT

Approved for Public Distribution, Distribution Unlimited

12b. DISTRIBUTION CODE

13. ABSTRACT *(Maximum 200 words)*

In phase I of this project, the applicability of the cone kernel time-frequency representation (CK-TFR) to underwater acoustic signal analysis was explored. The Cohen class of time-frequency distributions is described and the theoretical basis for improved resolution in the time-frequency plane is presented. Several examples are given of relative performance between members of the Cohen class, including the spectrogram. Specifically, the Wigner-Ville, Choi-Williams, CK-TFR, and spectrogram are compared. Improved performance with the CK-TFR prompted further study with actual acoustic signals. Biological and diesel surface vessel acoustics were analyzed with the CK-TFR and both a narrowband and broadband spectrogram process. Results favored the CK-TFR when compared in terms of T-F cell resolution, estimation of the signal's region of support, and detection statistics. The later were computed for a synthetic active sonar case with closely spaced (range and Doppler), multiple highlights in white Gaussian noise. Although, it is pointed out that the CK-TFR is sub optimum in this case. A signal processing workstation is defined which provides the means to conduct extensive tradeoffs between the CK-TFR and spectrogram process.

14. SUBJECT TERMS	15. NUMBER OF PAGES
Signak Processin; Frequency Analysis LOFAR Transients Acoustic Analyzer Spectrogram Time-Frequency Sonar Whale Calls	57
	16. PRICE CODE

17. SECURITY CLASSIFICATION OF REPORT	18. SECURITY CLASSIFICATION OF THIS PAGE	19. SECURITY CLASSIFICATION OF ABSTRACT	20. LIMITATION OF ABSTRACT
UNCLASSIFIED	UNCLASSIFIED	UNCLASSIFIED	UL

NSN 7540-01-280-5500

Standard Form 298 (Rev 2-89)
Prescribed by ANSI Std 239-18
298-102

BLANK PAGE

Table of Contents

BLANK PAGE

SUMMARY

This SBIR Phase I project has focused on the applicability of time-frequency representations (TFRs) to underwater acoustic signal analysis. Specifically, a preliminary comparative analysis was conducted with the cone kernel time-frequency representation (CK-TFR) and both wideband and narrowband spectrogram processors. After showing the theoretical foundations for potential improvement in resolution offered by the time-frequency representations of the Cohen class, performance comparisons were made between several members of that class. Using multi-component signals as test cases, the Wigner-Ville distribution (WVD), the Choi-Williams distribution, and the cone kernel distribution were compared with the spectrograms. Results were compared on the basis of signal representation accuracy over region of support, production of interfering cross-terms, and spectral resolution. The cone kernel time-frequency representation performed as well as the WVD against signals with single components and outperformed both the WVD and Choi-Williams TFR in multi-component signal environments.

In order to provide suitable comparisons between the conventional, short-term Fourier transform (STFT) based spectrogram process and the cone-kernel TFR, three classes of acoustic signals were identified. These were passive acoustic transients, passive narrowband dynamic tones and tonal groups, and low frequency/low Doppler active returns. A total of six (6) test cases were developed using actual recordings of biological signals (transients and tonals) and diesel surface vessel signatures. Ambient backgrounds for these cases included surface noise and rain. Narrowband and broadband spectrograms were produced for these cases and were directly compared with cone kernel time-frequency representation. In all cases, the time-frequency representation offered superior results to the spectrogram. Results were produced in color enhanced image formats to provide examples of proposed display considerations in the Phase II project.

A signal processing testbed was defined in this effort in terms of functionality and hardware and software architecture. Because TFR information is highly graphical in nature, a testbed built on a graphics workstation was deemed appropriate. A SUN SPARCstation 2 host was defined as the backbone of the system with back plane mounted signal acquisition and DSP32-based digital signal processing capability to enhance TFR throughput. All hardware and development software tools are commercially available. Software development in Phase II will be focused on efficient implementation of the CK-TFR process and refining its output presentations to maximize operator effectiveness. In addition to testbed development, continued in-depth performance assessment of the cone kernel time-frequency representation of acoustic data is proposed. Availability of Navy target signature data (passive and active) for use in these analyses will be explored. It is felt that the use of actual target data will provide an additional degree of confidence in the final results.

INTRODUCTION

The use of time-frequency representations of data in underwater acoustics applications is wide spread. These representations have generally been the proucts of a spectrogram process and have provided a significant increase in understanding of the acoustic environment and the nature of man-made and naturally occurring signals within that environment. The work performed during this Phase I project has focused on new techniques for computing a signal's time-frequency representation (TFR) which offers improvement in both temporal and spectral resolution and significant reductions in spurious components or "artifacts" in the resulting representation. Specifically, this work has focused on the use of the Cone Kernel Time-Frequency Representation (CK-TFR) in passive and active sonar applications.

This project was divided into three (3) tasks. Task 1 addressed the definition of algorithm performance criteria and developed an estimate of the computational complexities of the algorithm in terms of overhead and data latencies. In Task 2, test data were defined and the initial application of the CK-TFR to passive signatures of biologics and surface vessels resulted in time-frequency data which offered greater detail than that produced by the short-time Fourier transform (STFT). In addition, initial work was begun on optimizing the visual presentation of this data in order to improve information transfer to the operator. This is particularly important as the CK-TFR has increased the amount of information present in the time-frequency domain. This work was presented at the Vienna, Virginia offices of Space Applications Corporation in the Task 2 Program Review on 14 July 1992. Subsequent to that review, Task 3 of the project has concentrated on the definition of a signal processing testbed which integrates real signal acquisition, artificial signal synthesis, TFR computation, detection performance analysis, TFR map image processing, and database management. This work has been performed in parallel with efforts to identify a Phase II sponsor. In the Phase II effort, we propose to build the testbed and perform comparative analyses on actual data using the CK-TFR and short-term Fourier transform based spectrogram.

The report begins with a Background and Assumptions Section which offers a brief synopsis of the current ASW mission and the potential threats which face today's U.S. Navy. These threats consist of both new adversaries and new theaters of operation which present considerably more difficult conditions to the ASW officer. As a technical backdrop for the discussion of unconventional processing which follows, the next section describes current approaches to acoustic detection and analysis. Both active and passive processing are addressed. Next, a brief tutorial on time-frequency representations and a discussion of the Cohen class of TFRs is offered. Specifically, the cone kernel time-frequency distribution is defined and its properties are described and contrasted with those of other members of the Cohen class, including the short-term Fourier transform. Acoustic Signal Analysis Results and Discussion summarizes the results of the analyses conducted during the course of this study in which the CK-TFR process was applied to actual passive acoustic signals of surface vessels, biologics and synthetic active sonar waveforms. These are compared directly with spectrogram products. The following section presents a set of proposed functional requirements for the unconventional signal processing testbed. This includes a discussion of man machine interface (MMI) requirements and also offers a candidate hardware suite definition for the testbed which satisfies the functional and MMI requirements. The conclusions section presents summary comments and concluding remarks including recommendations for Phase II.

BACKGROUND AND ASSUMPTIONS

The Navy's Evolving ASW Mission

Earlier this year the U.S. Navy's Chief of Naval Operations published a strategy paper which established the Navy's priorities and mission requirements for the 1990's and beyond. This was prompted, in part, by the results of the Gulf War and the recent demise of the Soviet Union. A portion of the paper quantified the potential threat to the security of the United States and its interests abroad in terms of possible conflict and adversary characteristics.

As the United States Navy responds to recent global events and adapts both tactically and strategically, specific mission objectives and assets must also adapt. As a result, the Navy is preparing to respond to spontaneous regional conflicts which may occur in any number of volatile regions separated by large distances and distributed over the globe. The combat theater is envisioned as a rapidly changing environment with multiple fronts requiring highly coordinated command, control and communications to orchestrate immediate responses to changing tactical situations. The threat is expected to be fast and his weapons reflect a sophisticated level of technological development.

Currently, ASW mission characteristics are significantly impacted by this threat definition. Regional conflicts imply intermediate depth ("gray water") and possibly shallow water ("brown water") encounters. Increasing likelihood of littoral region operations implies a generally more reverberant environment with increased contact frequency, and higher ambient noise and interference levels. Venues for confrontation with third-world adversaries are likely to be in-shore of the 100 fathom line. Major choke points such as the Straits of Gibraltar or Malacca are good examples. Regional extensions of continental shelf in the vicinities of the Arctic coast of Russia, the Gulf of Thailand, the South China Sea or the Sea of Japan are examples which exhibit applicable physical oceanographic features that must be considered. Obviously, the Middle East region waters of the Persian Gulf and Red Sea are of topical concern. Indeed, it is also mandatory to consider regional waters of the United States when presented with the above scenario given the possibility of terrorist activities levied directly at U.S. ports.

Foreign development of advanced weaponry and exportation of these weapons, specifically quiet diesel-electric submarines, to third world adversaries presents a very real threat to national security. Russia, Germany, the United Kingdom, France, and Sweden all export modern submarine vessels with relatively modern torpedo, anti-shipping, and fire control technology. Some of these vessels posses air-independent propulsion. An example is the German 209-type submarine which can operate submerges for extended periods of time. There are 30 of this type of submarine, or variations of it, in operation with third-world Navies. Indeed, as the sales of such weapons spread, it is anticipated that both detection and identification of friend and foe will become increasingly difficult.

The Acoustic Environment

Littoral and shallow water operations impose significant disadvantages on the use of acoustic sensors and weapons. The waveguide defined by the surface and bottom boundaries does not support a deep sound channel mode limiting detection ranges. Multipath conditions are difficult to accurately model and predict. Bottom characteristics play a more important role in

the ability to model sound propagation and thermal conditions can present very severe velocity profiles which all but eliminate the use of active sonar systems over even moderate ranges. In coastal waters bottom terrain presents special problems in ASW prosecution. Besides presenting significant false returns to detection equipment, bottom features such as ravines and sea mounts can provide protection from pursuit by offering acoustic shadow zones and places to hide. Surface generated noise levels are typically higher for a given sea state because of the increase in reverberation. In addition, increased shipping-based noise levels are higher over open water equivalent conditions for the same reason.

Accurate acoustic modeling of the shallow water environment is an area of renewed interest. There is a severe deficiency of shallow water acoustic data to use as the basis for model verification so it is anticipated that model development will be an area of active research and development for some time to come. Current ray mode based models will remain the mainstay of shallow water acoustic predictions until refined means can be developed to replace them. The effects of sub-bottom inhomogeneities, irregular bathymetry and the mixed (fresh and salt water) layer on propagation conditions are difficult to accurately model. Generally, the shallow water propagation channel can be characterized as a highly reverberant non-linear channel which exhibits severe multipath and is, in general, highly non-stationary.

Acoustic ambient noise consists of surface generated noise due to wind waves and rain. These noise components generally occupy the same spectral bands in shallow depths as they exhibit in deep water. However, the measured levels tend to be higher for a given sea state or precipitation level due to the proximity of the bottom and higher reverberation conditions. In addition, shipping traffic tends to be denser with the resulting background levels between 20 and 200 Hz persisting at higher levels than in the open ocean. Figure 1 depicts both the well known Wenz curves and a global map indicating shipping traffic densities along major coastlines. Under these rather adverse conditions future ASW sensor systems will be required to detect, localize, classify and track submarines and submersibles with (potentially) greater stealth than that exhibited by today's modern nuclear fleet.

Conventional Acoustic Detection and Analysis Approaches

Our Phase I study concentrated on passive signal processing. However, in a real sense, many attributes of an analysis technique which offers substantial improvement in a passive signal analysis application can generally carry over to the active side as well. If a sonar signal processing technique is to be considered an advancement, then it must offer improved performance in one or more of the following areas:

PASSIVE SONAR -
- Enhance Figure of Merit
- Provide New Signature Characteristics or Features
- Aid in Rapid Classification
- Extend Classification Automation to Reduce Operator Workload

ACTIVE SONAR -
- Improve Reverberation-Limited Performance
- Provide New Signature Characteristics or Features
- Aid and/or Extend Rapid Classification Automation

Passive sonar has been extensively used as a major element in the ASW sensor suite. Radiated acoustic target signature features which have been key contributors to the success of passive systems include narrowband tones and broadband signature components which underlay the dominant tonals. In addition, acoustic transients produced by high energy but relatively short events have played an important but secondary role in target detection and classification. These events include hatch closures, torpedo door operations, and hull popping. As acoustic propagation and ambient noise degrade transients become more important. High resolution representations of transient signals in the time-frequency plane may offer additional signal features not discernible in current Transient Acoustic Processor (TAP) systems.

A transient processor which decomposes the gated transient into a spectral representation is offered in block diagram form in Figure A-2. The process is fundamentally identical to spectrogram processing and suffers from the same shortcomings. The process relies on the accuracy of the response of a fixed bandwidth filter bank to a highly non-stationary signal. This approach unnecessarily penalizes both temporal and spectral resolution performance.

Narrowband tone tracking problems such as that performed in LOFAR processing may also benefit from improved time-frequency processing. Enhanced time-frequency resolution and improved energy localization (estimation accuracy) in the time-frequency plane enhances tracking accuracy of dynamic narrowband tones and tonal families. This can obviously improve overall processing gain of the detection process against frequency agile signature components.

LOFAR processing is also based on the application of fixed bandwidth filters to fundamentally non-stationary signals. Figure A-3 presents a functional block diagram of a LOFAR processor. In actual application, very narrow filters are used to determine line width or, equivalently, short term stability. Therefore, fixed narrowbandwidth filters must be employed for these measurements while broader bandwidth filters are centered on the tonals so that the tonal frequency may be tracked. A time-frequency representation which provides arbitrarily fine temporal resolution while optimizing spectral resolution based on a desired characteristic may be an ideal candidate for this process.

In active sonar processing, separation of closely spaced targets(or target highlights) or detection of a low Doppler target present the greatest challenge. In Figure A-4 a Doppler processor is shown in which an FFT filter bank is used to ascertain an estimate of Doppler on the return signal. Usually, a compromise must be made in the design of the filter bank. In the case of a slow target, range-Doppler tracking problem pre-set fixed frequency selectivity may be suboptimal for separating target from reverberation or separating target highlights. Again, the need to accurately ascertain instantaneous frequency is of paramount importance in this application.

In each of the above cases, a window-and-transform technique such as that used in the spectrogram does not best represent desirable features of the signal. The assumption that the signal is stationary during the interval over which the FFT is applied may be invalid.

In the following sections, a description of the Cohen class of time-frequency representation is provided. Specifically, an entry in this family of signal representations which shows considerable merit in real applications is the Cone Kernel Time-Frequency Representation. Results of applying this technique follow the technique description.

TIME-FREQUENCY REPRESENTATIONS

The best and most common example of a joint time-frequency distribution is the short-term Fourier transform. It is expressed as,

$$S_t(f) = \int_{-\infty}^{\infty} h(t'-t)s(t')e^{-j2\pi ft}dt'$$

and the joint distribution is defined as the squared-magnitude, $P(t,f) = |S_t(f)|^2$. This is not the only representation nor is it necessarily the best. The spectrogram is sometimes described as a window-analyze-shift operator. The windowing operation, described by h(t) in the above expression, directly affects the results as can be seen by the example shown in Figure A-5. In this Figure two spectrograms are depicted. Both are representations of the same utterance of the word "joy". On the left side, the spectrogram has been performed with a relatively long window. On the right, the spectrogram has been performed with a short window. The results are predictable with the narrowband spectrogram (long h(t)) depicting fine spectral resolution with virtually no temporal detail. On the other hand, the wideband spectrogram (short h(t)) presents considerable temporally separated structure with only course structures in the spectral dimension.

The spectrogram is inaccurate for both cases. It overestimates duration events due to window smearing and overestimates bandwidths. It can also underestimate sweep rates as we shall see later. The STFT dose not jointly represent time-frequency structure. The quasi-stationary assumption generally leads to inaccuracies. A second example shows the effect of the time versus frequency tradeoff of the spectrogram.

Figure A-6 depict narrowband and wideband spectrograms of five exponentially decaying sinusoidal pulses. The pulses are shown in the top plot. The middle plot of the narrowband process clearly shows the strong fundamental frequency of the sinusoids and the peak sidelobes of the exponentially weighted pulse. But the actual time over which the pulse train exists is overestimated. The wideband spectrogram represents an accurate estimate of the temporal characteristics by clearly delineating each pulse in time. However, the spectral details of each pulse are severely under-resolved.

As a second example of the effects of the time-frequency tradeoff, a very important application is illustrated in Figure A-7. In this case, the slope of a swept tone produced by a chirped resonator must be estimated. Clearly, neither the narrowband or wideband spectrogram processor perform well. In the narrowband case in the top plot, the frequency components form a very "hazy" image of the up-chirp. However, the wideband spectrogram representation also confuses the estimate by presenting a fairly broad depiction of the up-chirp in the frequency dimension. The circles seen in the WB spectrogram in the bottom plot are the result of a the phase discontinuity at the end of one pulse and the beginning of a following pulse in the five (5) pulse train.

It was recognized some time ago that the fundamental limitation of the window-analyze-shift process is that imposed by the uncertainty principle. However, if windowing is not performed, then the uncertainty principle does not apply. To better understand this statement consider the spectrogram kernel in the (t, τ) plane. Figure A-8 shows a rectangular window and the

development of the kernel's region of support in the (t, τ) plane. The spectrogram kernel is described as $h^*(t+\tau/2)h(t-\tau/2)$. The rectangular window is shown in Figure A-8 in the upper left corner. The window, h(t), is shown in the upper left corner. The shift by $-\tau/2$ skews the region of support as shown in the lower left corner. Finally, a shift by $\tau/2$ skews the region in the opposite direction and the product of $h^*(t-\tau/2)h(t+\tau/2)$ is depicted as a black region in the bottom lower corner of Figure A-8. The black diamond is the region of support for the kernel and it clearly shows the dependence of the support intervals on both axes as a function of T. Therefore, as T (the window length) is varied, the support intervals vary also.

We use this above case as an introduction to the Cohen class of time-frequency representations [1]. In general, the Cohen class of TFRs uses an "arbitrary" kernel. The choice or definition is usually driven by the desired properties of the kernel. These will be discussed directly. The generalized TFR may be expressed as,

$$P(t,f) = \int_{-\infty}^{\infty}\int_{-\infty}^{\infty} \phi(u-t,\tau)s(u+\frac{\tau}{2})s^*(u-\frac{\tau}{2})e^{-j2\pi f}dud\tau$$

Here, $\phi(t, \tau)$ is signal independent for bilinear forms of the above expression. Recall that the spectrogram kernel can be any window function that can be expressed as an analytic function. Other possible kernel choices and their regions of support are presented in Figure A-9. In A-9(1), a function defined only on the τ axis is described by $\phi_W(t, \tau) = g(\tau)\delta(t)$. This kernel is the basis for the well known Wigner-Ville distribution. In A-9(2), the cone kernel defined by Zhao, Atlas and Marks [2] is described as $\phi_{ck}(t, \tau) = g(\tau)\text{rect}(t/\tau)$. The reason for its name is apparent in the shape of its region of support in the (t, τ) plane. The important point here is that the Wigner-Ville kernel and cone kernel exhibit a temporal resolution which is independent of T. Unlike the spectrogram kernel, T may be chosen without affecting temporal resolution. The marked difference between these two kernels is in the degree of cross-term generation in their respective time-frequency representations.

Desirable properties of TFRs may be described in terms non negativity, the distributions marginals, and the degree of support provided by the distribution. Non negativity ($P(t, f) \geq 0$) is desired for any bilinear joint distribution used in signal analysis as it implies that there is no "negative energy" represented by the distribution. This property also prevents nonsense results when distribution statistics are computed such as the spectral variance of a signal at a specific instant in time, i.e. $\sigma_f^2(t_0) \geq 0$. A joint distributions marginals describe the ability to produce either individual distribution from the joint distribution,

$$\int_{-\infty}^{\infty} P(t,f)df = |s(t)|^2 \text{ and } \int_{-\infty}^{\infty} P(t,f)dt = |S(f)|^2$$

A distribution's marginals and non negativity have a direct relationship on its ability to approximate exact start and stop times of a signal. In a previous example (Figure A-6), the spectrogram exhibited poor performance for both narrowband and wideband cases. Finite support properties describe a distributions behavior in terms of strong or weak. In general, it is highly desirable for the distribution to be zero when the signal s(t) is zero. Similarly, it is also desirable for the distribution to be zero when the signal's spectrum S(f) is zero.

Figure A-10 compares the finite support properties of five (5) TFRs. A synthetic signal was constructed of two sinusoidal waveforms, each operating at a different frequency. The top trace of the Figure illustrates this signal. Two pulses were constructed from these. The first pulse was formed with the addition of both sinusoidal waveforms operating over the same interval with both turning off simultaneously. This pulse period is approximately 15 milliseconds long. After a brief dead period of about 5 milliseconds, the lower frequency sinusoid turns on, then 5 milliseconds later the higher frequency sinusoid turns on. Both remain on for approximately 15 milliseconds and then both turn off simultaneously.

The wideband (WB) and narrowband (NB) spectrograms both error in depicting signal turn on and turn off events. The NB spectrogram representation depicts very early and very late signal transitions. Alternately, the WB representation is more accurate in depicting transitions, however, the 15 millisecond dead band does not appear due to energy "leakage" during this interval. The three Cohen class representations offered in the next three traces are the Wigner-Ville (WV). Choi-Williams (CW), and Cone Kernel (CK) representations. The Choi-Williams TFR has been included in these comparisons because of its use in speech processing applications. All three of these TFRs present strong finite support with all transitions in the time dimension closely aligned with those of the actual synthetic signal's. However, it should be noted that severe interference is apparent in the WV and CW TFRs at the frequency centered between those of the two sinusoids. The CK-TFR does not exhibit this interference. The interference in question is produced by the cross-terms of the bilinear distribution. This is a well known and well understood artifact of the Cohen class of TFR. The CK-TFR suppresses these terms while still providing the benefit of strong finite support. When more than one frequency component exists simultaneously in the analyzed signal, cross-term interference is produced.

A second example is offered in Figure A-11. In this case a non-stationary tone is analyzed by the same five (5) TFRs used in the previous example. The signal is a constant envelope sinusoidal pulse whose frequency linearly ramps between the starting and ending frequencies in the center of the pulse. The time-series of the pulse is shown in the top trace of Figure A-11 and the ideal time-frequency trajectory is indicated in the bottom trace. The NB spectrogram representation again poorly estimates the start and end of the pulse. The frequency ramp is completely absent in this case. A better result is obtained with the WB spectrogram, however the pulse duration is slightly overestimated and the slope of the frequency ramp is not estimated well. The WV-, CW-, and CK-TFRs indicate pulse duration and the frequency ramp quite well. However, the interference terms are stronger in the Wigner-Ville and Choi-Williams representations.

It is reasonable to question whether there is true improvement in using a time-frequency representation which does not make use of the window-analyze-shift approach. The previous synthetic signal cases imply that there are indeed possible improvements which may be appreciated by these time-frequency formulations, especially the cone kernel TFR. The CK-TFR reduces cross-term interference to a greater degree than the Wigner-Ville or Choi-Williams TFRs and is therefore better suited for use with signals that are more complicated than single tones against a low background. Artifact suppression is better in the CK-TFR and spectrogram than other time-frequency techniques.

Table A-1 presents a summary of the most important properties for the four (4) TFRs discussed above. The CK-TFR optimizes time and frequency support and artifact suppression

at the expense of providing marginals and non-negativity. However, in applications where complex, multi-component signal analysis is required wherein accurate temporal and spectral transition estimates are require and "spurious" artifacts must be suppressed, then there is a strong case for the use of the CK-TFR over other candidates.

ACOUSTIC SIGNAL ANALYSIS RESULTS AND DISCUSSION

In task 1 of this project three classes of acoustic signals were identified as candidates for study during this Phase I effort. They are:

1. Passive Transients,
2. Passive Narrowband Dynamic Tones and Tonal Groups, and
3. Low Frequency/Low Doppler Active Return.

In each case there are basic similarities describing the nature of these signals. All are non-stationary with varying signal epoch duration. Transients are relatively intense with a complex temporal and spectral structure. As a result, these signals are potentially very rich in classification clues. Dynamic tones and/or tonal families may vary in intensity, but the nature of these signals is relatively well structured. Frequency variations may occur quickly or slowly depending on relative target motion. Spectral line width provides classification clues and individual line relationships with each other also are used for target identification. Thus, there are conflicting requirements to provide both an estimate of line width (short term frequency stability using very narrowband estimation filters) and identification of tonal families which may span several octaves. These tasks are usually performed independently. Finally, the active sonar case is of obvious interest if a sonar processor must operate against low Doppler targets without the use of chirp processing (reverberation whitening and matched filtering).

With these cases in mind Space Applications Corp. and System Engineering Technologies, Inc. recorded the following data sets for use as study cases with the CK-TFR process:

1. A single whale feeding click with a background composed of natural ambients and a single screw fishing boat. (Passive Transient)

2. A single whale call with a background composed of natural ambients and a single screw diesel fishing boat. (Passive Dynamic Tonal Family)

3. Distant diesel fishing boat with propeller vortex noise against a low ambient noise background. (Passive Stationary Tonal Family at Low SNR)

4. Close diesel engine noise with propeller vortex noise in against a low ambient noise background. (Passive Stationary Tonal Family at Moderate SNR)

5. A combination of an actual whale call and propeller cavitation with synthetic background ambient noise. (Example of synthetic signal generation proposed for Phase II workstation)

6. Simulated active sonar return of three point scatterers closely spaced in range and Doppler. (Active Resolution Test Case)

Each case was analyzed with three (3) processes: the CK-TFR, a wideband spectrogram processor, and a narrowband spectrogram processor. In each case a time-frequency map was produced, the levels were quantized and false colorization was applied. Actual colors used to represent specific levels were varied to investigate candidate schemes for optimum contrast. The results presented in Appendix A show four (4) sections in each Figure. The top section is

a time-series plot of the signal section analyzed. The next section below is the cone kernel TFR output. The section below that is the wideband spectrogram and the bottom section is the narrowband spectrogram. Signal times and frequencies are labeled for each. The real acoustic data was recorded at Behm Canal in southeast Alaska. Background ambients all contained noise due to wind waves and moderate rainfall. The biologics recorded on these records are believed to be an Orca whale pod feeding on salmon with more than one individual represented in this set of records. The data was taken off of a single-channel recording system aboard a Minimet buoy. The hydrophone was located at a depth of 60 meters. The data was recorded on digital audio tape and processed in the Interactive Systems Design Laboratory at the University of Washington. Signal synthesis and editing was performed in the Signal Analysis Laboratory at Space Applications Corporation. Acoustic synthesis was performed using a "SoundBlaster Pro" digital acquisition, processing and synthesis system. An 80386 host was used in conjunction with this system to produce the synthesized ambients in case 5.

Figure A-12 presents the time-frequency representations of case 1, a whale feeding click with a single screw in the background. Clicks are produced by the whale for high resolution range finding as the whale makes its "final approach" on its quarry. High levels are represented blue and low levels are green. Red information lies in-between these extremes. The time-series shows a series of pulses in the center of the record. Colored magnitude maps show the increase in energy at this time, however, the NB spectrogram map at the bottom exhibits poor finite support and corresponding inaccuracies in estimating the beginning and end of the event as expected. While the WB spectrogram in the third section does a better job in localizing the event in time, the frequency resolution is notably reduced. The CK-TFR indicates a strong central frequency component during the event just below 1000 Hz. This corresponds to the basic repetition frequency of the pulses. In addition, temporal localization is slightly better than the WB spectrogram. It should also be noted that the CK-TFR has placed the most of the background energy below 1000 Hz. Whereas the NB spectrogram indicates moderate levels across the entire displayed 4 KHz band. No pre-whitening of the data was performed, therefore, the CK-TFR representation is accurate due to the dominance of ambients at the lower frequencies.

In case 2, a single whale call was analyzed. This event was approximately 0.5 seconds long and its time-series is offered in the top section of Figure A-13. SNR was relatively high and was estimated to be approximately 15 dB during the peak (center) of the call. In these photographs, yellow is used to represent the maximum level and red is minimum. The dark tones are interim levels. As the CK-TFR indicates, the call actually consists of a family of discrete tones separated in frequency by a fixed offset. This offset appears to remain fixed even during the frequency trajectory which appears as an arc in the TFR. The NB spectrogram also depicts the same number of components but they tend to be broader in spectral width. Note that the NB spectrogram does not smear the event in time as badly as it did the clicks in the previous case. The WB spectrogram underestimates the number of tones and can not offer the same spectral resolution that either of the other two processes possess. Again most of the acoustic background is isolated to frequencies below 500 Hz in the CK-TFR. The screw components consisting of cavitation and hub noise were below the ambients in this case with an estimated SNR of -10 dB. In the following case, these are analyzed under more favorable conditions.

Case 3 represents the acoustic signature of a distant diesel fishing boat in-transit across Behm Canal in relatively low ambients. The estimated SNR of the boat's signal under these

conditions varied between -6 and 0 dB and its time-series is depicted in the top section of Figure A-14. The WB spectrogram is devoid of any trace of the boat's signature. In this case, the expected signature consists of the 60 Hz family of harmonics produced by the diesel engine. The NB spectrogram exhibits some tonal content, particularly around 180 (at 8.1 seconds) and 540 Hz (8.3 to 8.4 and alternately fading thereafter). Tonal lines are clearly evident in the CK-TFR map at these frequencies over most of the record.

In order to show the details of the CK-TFR map more clearly, case 4 was chosen as an example of how the CK-TFR can produce very high resolution maps over a large contiguous band of frequencies. Figure A-15 presents this case in point. A relatively high SNR condition was captured with a diesel fishing boat. SNR conditions varied, but generally remained above 15 dB over the 2.6 second record. In this Figure, the spectral lines produced by the diesel are clearly evident in the CK-TFR map around 120 and 180 Hz. The spectrograms do not present comparable images. In Figure A-16, half-band expansions of the same data indicates the NB spectrogram (on the left) does indeed indicated a tone around 360 Hz (the large yellow band). The CK-TFR (on the right) indicates considerably finer detail with 60 Hz family lines clearly depicted at 60, 120, 180, 240, and 360 Hz. Above these frequencies the signal falls below the background. These detailed maps were not produced by rerunning the processes over the same data with greater spectral resolution, these maps are the results of zooming in on the low frequency region of those maps presented in Figure A-15.

Case 5 offers the last example of passive acoustic signal analysis, although it is a special case. Here, we combined the actual recording a whale call and nearby shipping with synthetic background noise. Rain noise was simulated which produces a flat hump in the spectrum centered around 1200 Hz. The actual acoustic signals were captured under high SNR conditions and the noise was eliminated from their record. The synthetic background was added to the "signal-only" record to produce a composite under controlled SNR conditions (15 dB peak). The CK-TFR in Figure A-17 indicates a fairly flat background (mostly red) with the whale call appearing between 5.0 and 6.0 seconds and reverberation following (yellow indicates high level). The spectral content of the call includes fairly constant tonal components at 1200, 1800, and 2400 Hz after and initial rapid down-chirp. It is also obvious that there is a high noise trend in the noise below 300 Hz over much of the record. This is due to the combination of the low frequency 1/f ambient noise model included in the synthesized data and the presence of a diesel tonals. As has been the case in the past examples the NB spectrogram indicates less resolution because the levels are generally high across the band (greater density of yellow). This indicates a greater equivalent noise bandwidth in the NB spectrogram than in the CK-TFR.

The last case studied in our Phase I work was the application of the CK-TFR to an active sonar return. This case was also reported by Atlas, Loughlin, Pitton and Fox [3]. The sonar data was synthesized by modeling three (3) point scatterers separated in range and Doppler by 10 range frames and 15 Doppler bins, respectively. The pulse was designed to have low frequency sidelobes below the detection threshold. Figure A-18 depicts the Doppler map produced by three (3) processes. Figure A-18(a) is the ideal Doppler map. Figure A-18(b) is the map produced using the conventional cross-ambiguity function. Figures A-18(c) and (d) are the Wigner-Ville Distribution (WVD) and CK-TFR Doppler maps. In this noiseless case all three exhibit the presence of all three targets. The cross-ambiguity function offers the least frequency resolution and it also smears the return in range. The WVD appears to provide the greatest Doppler resolution, however, the cross-terms produce significant interference on top

of the center target making it also appear as an interference artifact. The CK-TFR has accurately estimated the range extent of each return and has significantly reduced interference terms. Figure A-19 (a), (b) and (c) present the same sonar model with white Gaussian noise added to the process. SNR was adjusted so that the peak return amplitudes were equal to the rms noise level. As one might expect, the conventional cross-ambiguity function method resulted in a map with marginally detectable returns (probability of detection < 20%). The WVD Doppler map produced artifacts which were detected as targets and also resulted in the loss of the center target. Finally, the CK-TFR produced solid detections with high reliability (probability of detection > 95%). It should be noted, however, that the CK-TFR is not an optimal detection process like the matched filter processor is in the classic case where the signal is composed of the target return and additive white Gaussian noise.

The results of the preliminary analyses conducted during Phase I of this effort and exemplified by the above six (6) cases may be summarized as follows:

- Significant improvement in time-frequency cell resolution was provided by the CK-TFR over the NB spectrogram.

- The CK-TFR produced significantly lower artifact or interference levels than the Wigner-Ville or Choi-Williams TFRs in cases where the signal analyzed was multi-component in nature.

- The CK-TFR produced a greater amount of time-frequency structure than produced by the NB spectrogram when applied to signals composed of either stationary or non-stationary (dynamic) frequency components.

- Potential improvement in Doppler sonar detection performance was exhibited by the CK-TFR process in marginal SNR conditions over conventional cross-ambiguity processing and the Wigner-Ville distribution. Although the CK-TFR is not an optimum detection process like the matched filter in the case analyzed in this study.

Also in this analysis, areas of practical concern such as displays and custom acoustic signal synthesis were addressed:

- Qualitative assessment and development of the TFR map display to enhance intelligibility and operator performance must be addressed in as a component of further work in Phase II.

- Combining real and synthetic underwater acoustic signal components was verified, thereby supporting the proposed approach for the Phase II workstation.

Given the above results regarding the potential benefits offered by of a CK-TFR based acoustic processor, the remaining task (Task 3) in the Phase I effort was addressed. In this task the requirements for a Phase II testbed were developed and a recommended hardware and software suite were identified. The following sections provide the results of this task.

SIGNAL PROCESSING TESTBED FUNCTIONAL REQUIREMENTS

Phase II of this work will be composed of two tasks. First, a signal processing testbed will be implemented and second, using this testbed, the CK-TFR algorithm will be characterized in terms of its competitive performance against short-term Fourier transform (STFT) based processing like the spectrogram and LOFARgram. A functional block diagram of a signal processing testbed which we feel will accomplish this is offered in Figure 1.

Signal acquisition and audio generation are both important functions of the testbed. These operations are indicated in the upper left-hand corner of the Figure. Functional data flow and operation from the signal digitization process to display proceeds as follows. Actual acoustic signals are passed through a signal conditioning process which amplifies and applies anti-alias filtering. Analog-to-digital conversion is performed which samples, quantizes and digitizes the signal. The digital signal is buffered and, ultimately saved on disk. At this point the digital signal or time-series may be viewed directly through the Display and Data Control Module, passed out through signal reconstruction for audio presentation, processed in the Time-Frequency Processing Module, or used as a signal component in the Data Synthesis Module. Each module identified in Figure 1 is a software module which performs specific operations independently. The following paragraphs describe the operation of each module in detail.

Data synthesis is defined in our application as the generation, through numerical means, of artificial signal components such as passive and active acoustic signals, noise and interference, and the combination of these components in a predetermined fashion with actual recorded signals. The capability of mixing real and synthetic signals, while controlling their relative levels, offers a powerful technique to controlling specific signal parameters. Defining and building specific signal characteristics will be an important feature for evaluating processing performance of the CK-TFR technique. As Figure 1 indicates, the Data Synthesis Module contains two (2) types of synthesizers. The first is a noise generator capable of producing white or colored Gaussian noise and noise with arbitrary noise power spectral density. The last function is useful in simulating various shipping and rain conditions. The second synthesizer produces a variety of coherent signals including continuous wave (CW) generation, linear and hyperbolic signal formats, exponentially decaying transient pulses, and the ability to produce auto regressive-moving average based signal models. The last signal type becomes important for generating complex signal spectra which include many discrete frequency components in a very efficient manner. Amplitude weighting and combining the synthetic noise and signal components is performed under the control of the Data Synthesis Module's own configuration and control program. Selection of the desired signal and noise elements and definition of their relative levels is performed simply on a per sample basis because all noise representations are considered additive. The resulting synthetic signal may be archived or combined with real data stored on disk. This weight and sum process in also under control of the Data Synthesis Module. Synthetic or composite (real plus synthetic) may be sent to both the pre-processed signal time-series display or to signal reconstruction for audio presentation.

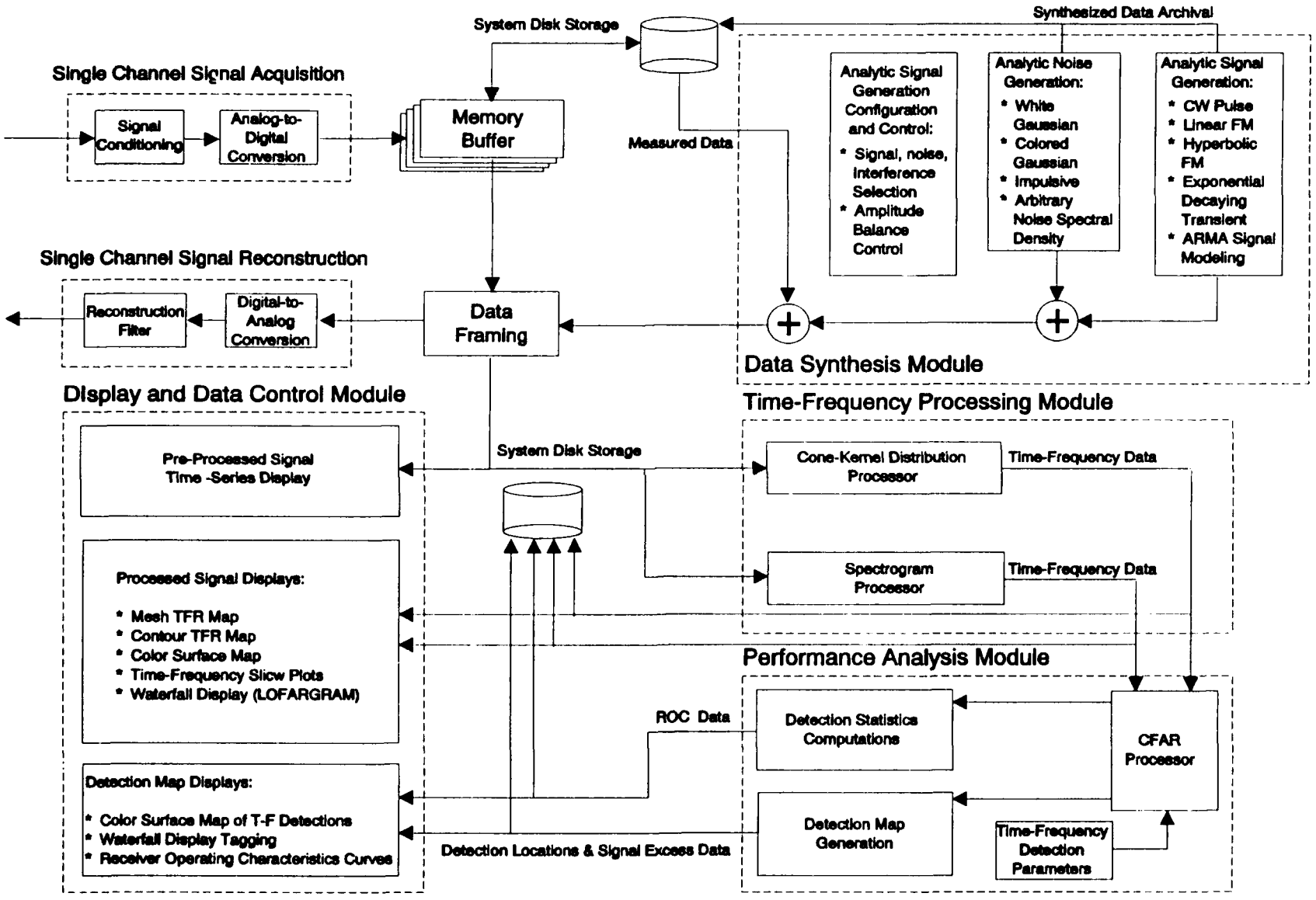

Figure 1 Signal Processing Testbed Functional Block Diagram

The Time-Frequency Processing Module contains both the CK-TFR and STFT processors. They both operate on the same signal which is selected by the operator and their output products are both identical in numerical format. The input time-series is real to conserve storage space. As a time-series record is processed by these operations, a frequency vector containing complex (amplitude and phase) estimates of the instantaneous frequency content of the signal is produced for each sample. The processors use wraparound techniques on the data at the beginning and end of each record. When the entire record has been processed a matrix of complex data whose dimensions represent time and frequency will exist for each processor. A continuous 20 second record will produce an output matrix of data spanning a 4 KHz band of 640 million entries (1 Hz cells assumed). With each entry represented by a 32 bit floating-point word that matrix would require over 2.5 gigabytes of storage. In our testbed concept, the operator will review the signal both visually and aurally so that data framing may be applied. The selected frame will be relatively small, usually on the order of 0.5 seconds and spectral cell width will be selected in conjunction with the theoretical resolution of the processor. This approach was used in our Phase I effort and we found it to be an efficient means of controlling the data processing operations.

In Appendix A, Figure A-20 depicts the general approach for computing the CK-TFR. Prior to this process the time-series must be Hilbert transformed to produce a complex and analytic representation of the signal (only positive frequencies). In addition, the time-series must be pre-whitened if LOFARgrams are to be produced with the CK-TFR output map. The STFT processor is constructed as a conventional spectrogram processor with a sliding time-series window selecting the FFT frame. Usually, an FFT is not computed at every data point. A percentage overlap between frames is incorporated in the algorithm and this may be subjectively based on the dynamics of the time-series itself. Control of processing parameters such as the CK-TFR α parameter which controls the slope of the cone kernel and percent overlap in the STFT processor are under the control of the Time-Frequency Processing Module. This is not indicated in Figure 1. Time-Frequency Processing Module outputs are stored and made available to the Performance Analysis Module and the Display and Data Control Module.

Performance analysis has been defined by the Navy for this study. It was recommended in the Program Review on 14 July that the CK-TFR process should be evaluated in terms of its Receiver Operating Characteristics (ROC) and resolution as observed in target detection maps. Therefore, the Performance Analysis Module includes the ability to make performance assessments based on these characteristics. ROC curves are produced by plotting probability of detection against the probability of false alarm. Usually a family of curves is produced describing performance as a function of SNR. Using a Constant False Alarm Rate (CFAR) processor operating directly on the TFRs, SNR, probability of detection (Pd) and probability of false alarm (Pfa) will be computed. Detection threshold will be varied and detection statistics will be accumulated using Monte Carlo techniques. Detection maps can be generated which depict Pd and Pfa levels in specific time-frequency or range-Doppler cells. In addition, signal excess information can also be represented in this manner. Signal excess is the difference between the received level in a cell and the threshold level. ROC data and detection maps are sent directly to the Display and Control Module.

All displays are processed and formatted in the Display and Control Module. We intend to apply several image processing techniques to the raw time-frequency maps to investigate possible improvements in contrasting spectral features. As indicated in our Phase I proposal

we believe that TFRs are particularly well suited for further 2-D image processing techniques such as edge detection filtering. This processing is not indicated in Figure 1. There are three (3) types of displays currently envisioned. Pre-processed signals are displayed on a time-series display which permits zooming in on specific frames over large time-series records. These may be represented in linear amplitude or decibel scales. The second type of display group is called the Processed Signal Displays. These displays include the following:

- Three-dimensional wire or mesh plots of TFR map magnitudes
- Two-dimensional contour TFR map
- Two-dimensional, color plot of TFR map magnitudes
- Two-dimensional Time-frequency (or alternately range-Doppler) map slices
- Waterfall display similar to a LOFARgram display

Each of these displays offers the operator the ability to visualize the data in a different manner. As indicated in the conclusions following the data analysis results section, we realize the importance of incorporating into Phase II a task to address display design. Color scaling the data properly can affect operator performance in a positive fashion. In each of the above displays the output maps produced by the T-F processors or slices of them may be produced in either 2-D or 3-D format. Rotation about three axes of the 3-D displays is a desirable feature to facilitate interpretation of the results. The color surface map is an "image" similar to the results presented in Appendix A . As mentioned earlier, these images can be post-processed to enhance signal trajectories in time-frequency space. These displays are used to present amplitude-only information. Both linear magnitudes and decibel levels will be supported.

The last type of displays produced by the Display and Data Control Module are the detection map displays. These include:

- Two-dimensional, color plot of TFR map detections indicating signal excess
- Waterfall display (LOFARgram) detection tags
- Two-dimensional Receiver Operating Characteristics Curves

Locations of detections and their corresponding signal excess levels will be indicated on a two-dimensional overlay which will have a cell-for-cell correspondence to the magnitude maps mentioned in the previous paragraph. In a similar manner, the waterfall magnitude map described above will be augmented by a detection tag overlay produced by this module. Finally, ROC curves will be produced within this module. Display and data control implies some kind of man-machine interface or MMI. Our concept is discussed briefly in the following section.

Man-Machine Interface and Software Development Environment

One driving requirement for our testbed concept is to be able to implement the basic system using commercially available hardware and software components. With this in mind, and the

desire to maintain a degree of compatibility with Navy equipment such as the standard shipboard desktop computer system DCS-2, our testbed will be built around a SUN SPARCstation 2[R] workstation. The working software environment will be UNIX based and SUN's OpenWindows[R] environment will be the programming environment. This core system provides the combination of versatility and expandability into a powerful graphics workstation. A prototype man-machine interface can be developed on this platform using a windows-based approach. This interface will be largely composed of individual functional modules or program segments which will look like separate control panels to the operator. Dynamic program linking will be supported in this environment so that the modules will transfer information between themselves in a seamless fashion. Space Applications Corporation provided a demonstration of this capability with their Modular Acoustic Signal Processing Tool (MAST) at the Program Review in July. Control panel operation is very similar to DOS windows applications. Operator interaction is performed with the keyboard and a mouse or trackball, ideally with the former taking a minor role.

Ideally, we hope to develop a prototype architecture for an advanced LOFARgram processor during a Phase II effort. We are not attempting to develop a real-time processing capability with this system. However, serious considerations will be given to making the displays and controlling functions as familiar as possible to a sonar operator. System Engineering Technologies, Inc. provides sonar operator expertise in their staff. An extension to this prototype MMI approach has been considered. In a follow-on development, a touch screen capability could be implemented further reducing the requirement for both the keyboard and mouse/track ball. In any case, a considerable amount of focus will be placed on optimizing efficient use of image information to improve acoustic signal interpretations.

Recommended Testbed Hardware Suite

The signal processing testbed will be composed of the following components:

1. SUN Microsystems SPARCstation 2GT Desktop 3-D Graphics System
2. DSP32-based digital signal processor (back plane mount)
3. Analogic AD/DA system (back plane mount)

Hosted on the Sun, the actual TFR algorithms will be implemented on a dedicated digital signal processor. Most of the algorithms intense computations are concentrated in the autocorrelation and FFT processing. In actual implementation, even the autocorrelations will be performed using the FFT algorithm. The DSP will be used to improve FFT throughput. Analog-to-Digital and Digital-to-Analog conversion will be performed on the back plane of the host computer as well. Since this is only a single acoustic channel system the required sample rate is relatively low. A 10 KHz band signal can be over sampled by a factor of 5 (5 times the Nyquist rate) and provide a high resolution time-series representation with a 100 KHz 16-bit A/D.

[R] Trademarks of SUN Microsystems, Inc.

CONCLUSIONS

Three (3) tasks were originally defined for phase I of this SBIR project . Specifically, these were to 1.) develop algorithm performance criteria and computing requirements, 2.) define a small but sufficient set of test data classes, and 3.) define a signal processing testbed for Phase II. These tasks have been completed successfully with the addition of completing initial side-by-side comparative studies with the cone kernel time-frequency representation and the short-term Fourier transform. The analyses were performed on at least one representative case from each class of signal type defined in task 2. Results from these analyses support the following conclusions.

Significant improvement in time-frequency map cell resolution was apparent in the reduction of equivalent noise bandwidth between the CK-TFR process over the NB spectrogram. This also contributed to an increase of signal structure apparent in the CK-TFR map over that observed in the NB spectrogram. The cone kernel process exhibited significantly lower cross-term interference levels than the Wigner-Ville or Choi-Williams TFRs in cases where a multi-component signal was analyzed. This was true regardless of the stationarity of the signal during the course of the analysis record. A simulated Doppler sonar case was designed with three closely spaced targets in range and Doppler under marginal (0 dB) signal-to-noise ratio conditions. Three processors were applied to this data, the conventional cross-ambiguity processor, the Wigner-Ville distribution and the cone kernel TFR. The CK-TFR range-Doppler map results were significantly better than the others. Specifically, the cross-ambiguity processor produced a probability of detection of less than 20%. The WVD produced significant cross-term interference which obscured one of the targets and produced many false alarms. The probability of detection for the CK-TFR was computed to be greater than 95% for the detection of all three targets. However, it was noted that the CK-TFR process is sub-optimal and theoretically performs poorer than the matched filter detector in this case.

In addition to the encouraging results from these analyses, a synthetic underwater acoustic signal generation methodology was demonstrated. Using a commercial synthesizer-signal processing board hosted on an 80386 PC, background ambient noise was produced. Actual whale and diesel engine acoustics were amplitude weighted and combined with the synthetic component to produce a custom acoustic signal test case. A refined implementation of this approach was described for the proposed signal processing testbed.

Qualitative assessment of candidate TFR map displays was identified as an important element in the next phase of this project. It was found during the course of the signal analysis work that even color range assignments to magnitude scales could have a severe impact on intelligibility. The windows environment and SUN's graphics application development tools were selected as the basis for a development system with which to refine the current displays.

Finally, a signal processing testbed architecture was defined in terms of functionality and recommended commercially available hardware and software components. Utilizing dynamically linked modules the testbed will perform signal acquisition and generation, time-frequency processing, performance analysis, and provide three categories of displays. Displays will present pre-processed time-series, T-F processed data, and detection maps. Performance will be evaluated in terms of detection statistics, ROC curves, time-frequency cell resolution, processing overhead, and feature extraction improvement.

All of the work performed thus far has been in preparation for a potential Phase II project which will focus on testbed development and in-depth CK-TFR performance characterization. In addition to this, considerable energy was spent developing materials which summarized our work to date for potential Phase II sponsors. The unusual format of this report reflects those efforts.

REFERENCES

1. L. Cohen, "Time-Frequency Distributions - A Review", Proc. IEEE, vol. 77, no. 7, pp. 941-978, July 1989.

2. Y. Zhao, L. Atlas, and R. Marks II, "The Use of Cone-Shaped Kernels for Generalized Time-Frequency Representations of Nonstationary Signals", IEEE Trans. ASSP, vol. 38, no. 7, 1990.

3. L. Atlas, P. Laughlin, J. Pitton, and W. Fox, "Applications of Cone-Shaped Kernel Time-Frequency Representations to Speech and Sonar Analysis", Transactions of the International Symposium on Signal Processing and its Applications, Gold Coast, Queensland, Australia, August 27, 1990.

Appendix A

This appendix contains the Figures referred to in the body of the text. These are in the form of viewgraphs as they were used as the means to report progress during the course of the project and as the basis for technical presentations to perspective sponsors.

UNCONVENTIONAL
SIGNAL
PROCESSING
SBIR

Coastal Zone Conditions are Characterized by Shipping and High Ambients

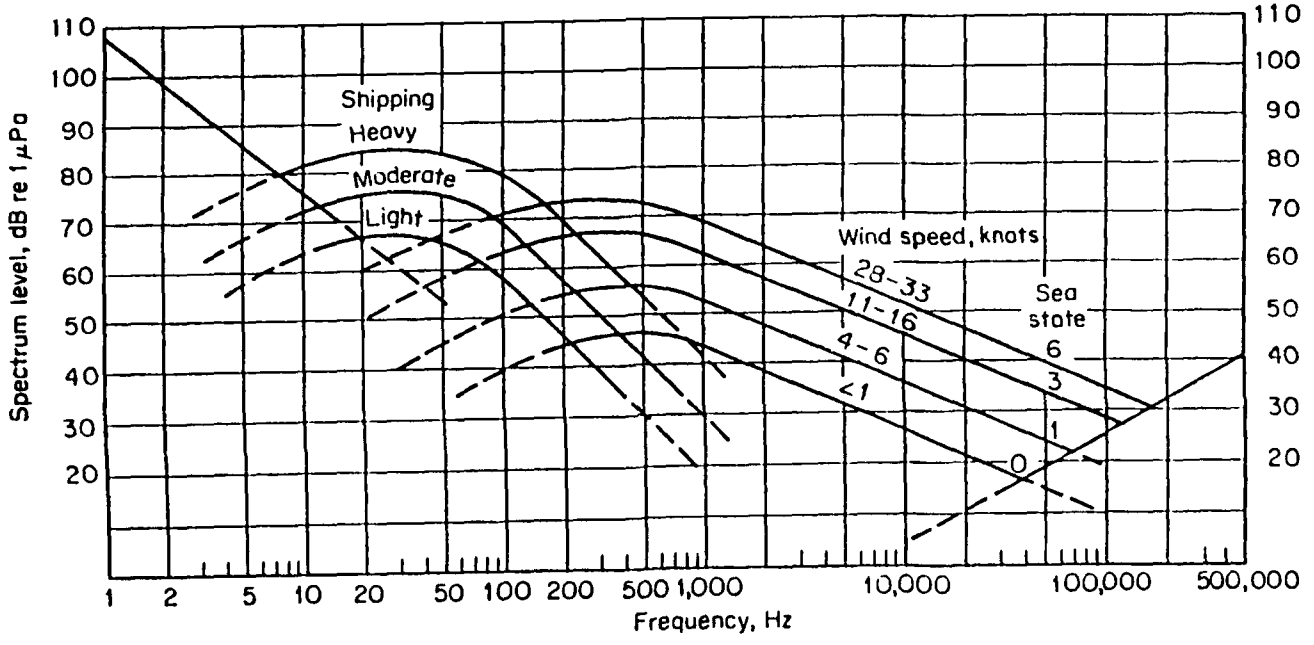

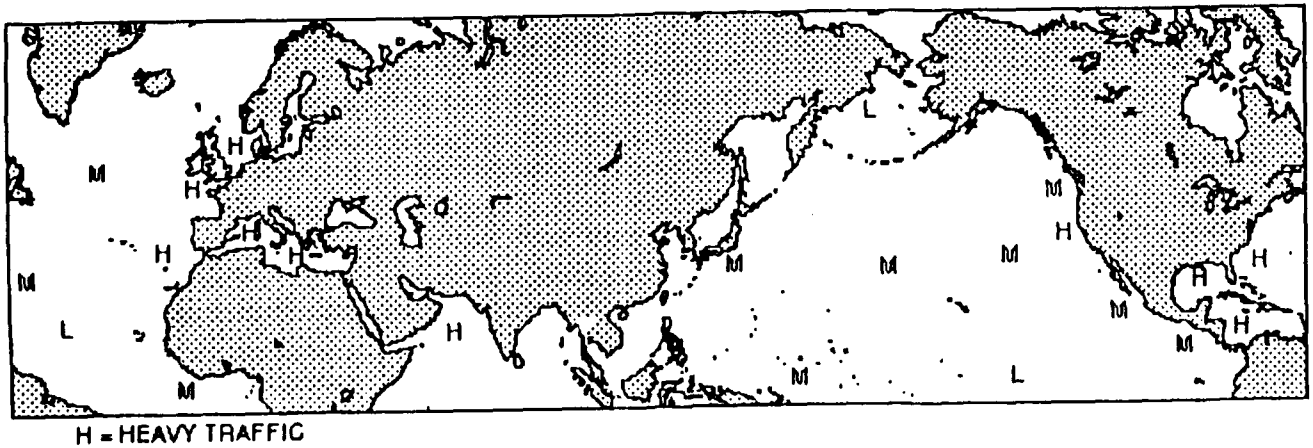

H = HEAVY TRAFFIC
M = MEDIUM TRAFFIC
L = LIGHT TRAFFIC

Figure A-1

V035.DRW

BLANK PAGE

Figure A-2

Transient Processing Shortcoming

Spectrogram Processing with Constant Frequency Resolution is Applied to Highly Non-Stationary Signals - Unnecessarily Penalizing Both Temporal and Spectral Resolution Performance

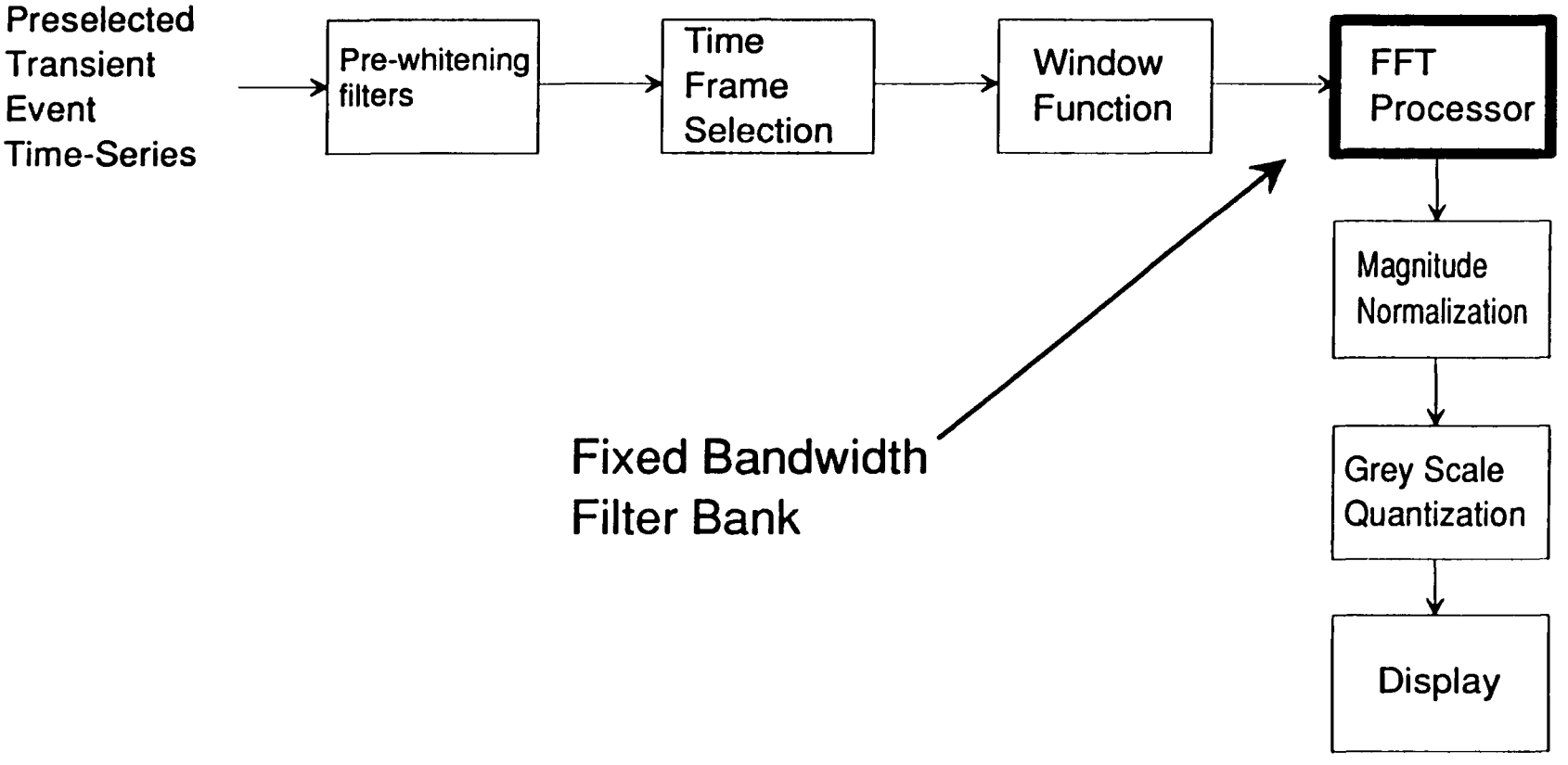

BLANK PAGE

UNCONVENTIONAL
SIGNAL
PROCESSING
SBIR

Figure A-3

Lofar Processing Shortcoming

A Variety of Fixed Bandwidth Filters Are Applied to Signals That May Have Non-Stationary Temporal and Spectral Characteristics

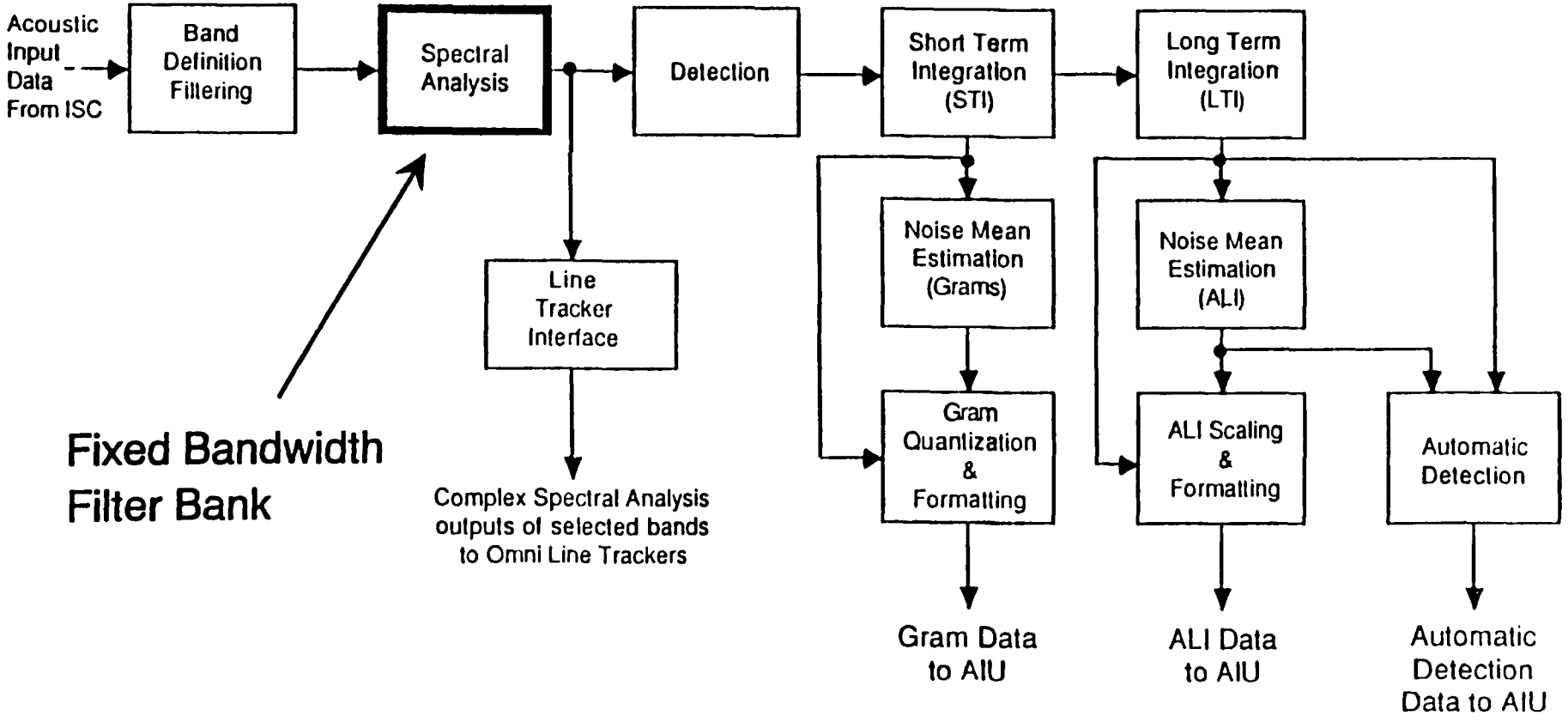

VG9.DRW

BLANK PAGE

Figure A-4

Active Processing Shortcoming

In the Slow Target, Range-Doppler Tracking Problem, Pre-Set Fixed Frequency Selectivity May Be Suboptimal For Separating Target From Reverberation or Separating Target Highlights

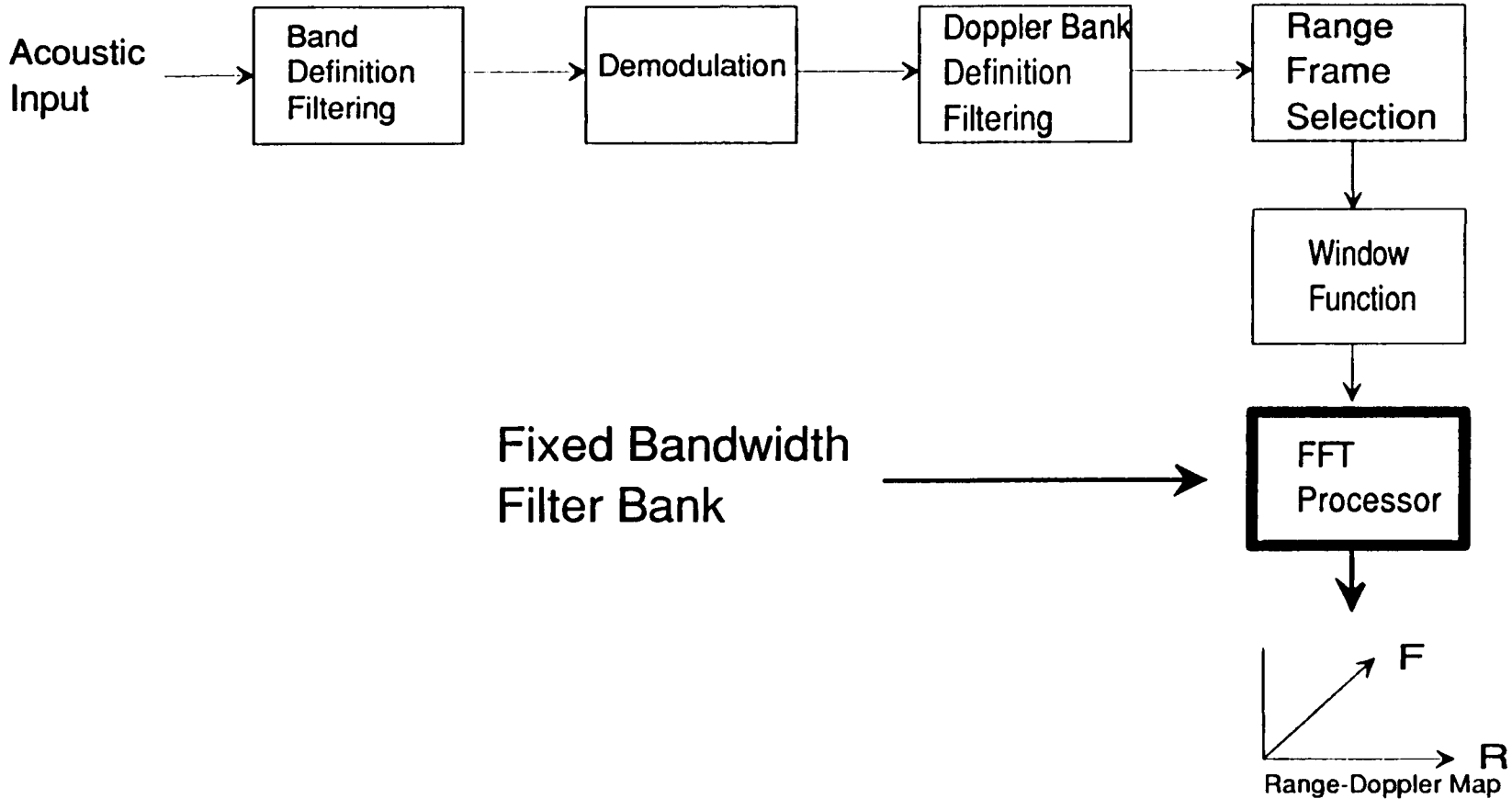

VG11.DRW

BLANK PAGE

UNCONVENTIONAL
SIGNAL
PROCESSING
SBIR

Figure A-5

Effect of the Window Length for the Conventional Technique

Narrowband Spectrogram (long $h(t)$): "joy"

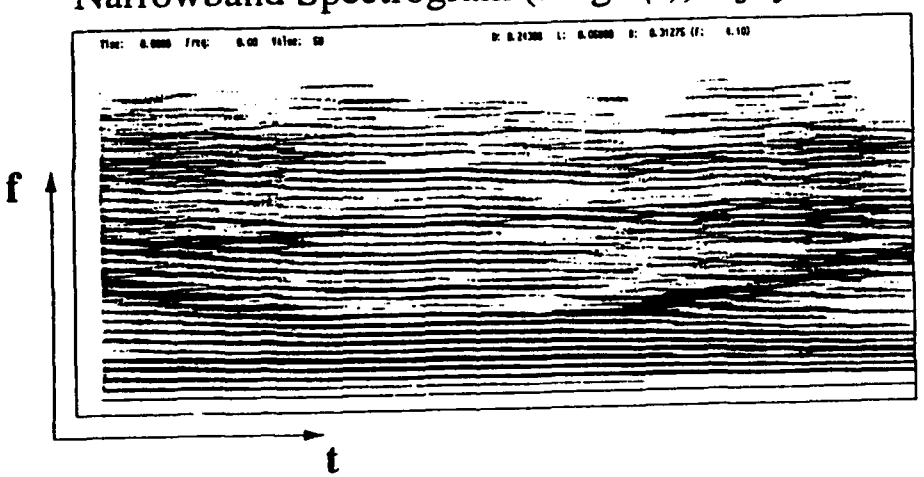

Wideband Spectrogram (short $h(t)$): "joy"

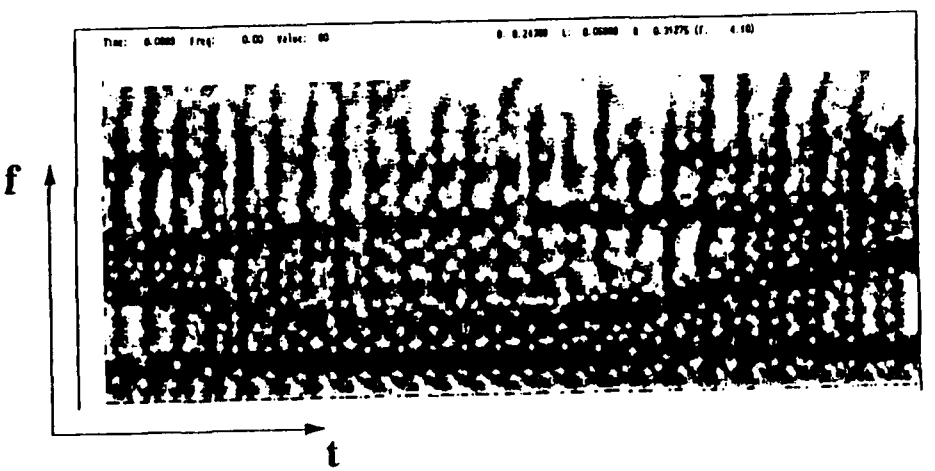

BLANK PAGE

UNCONVENTIONAL
SIGNAL
PROCESSING
SBIR

Figure A-6

Time Versus Frequency Resolution Tradeoff of the Spectrogram

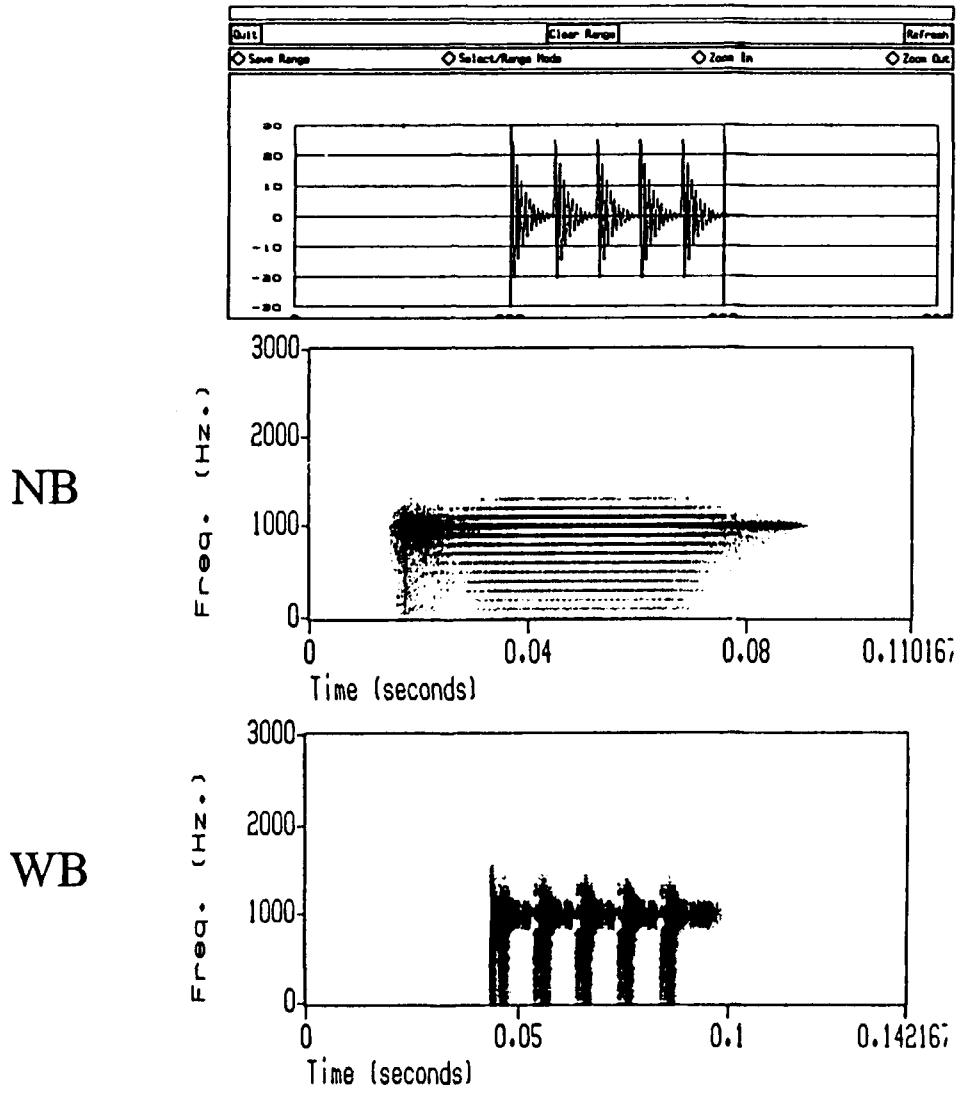

LE84.DRW

BLANK PAGE

Figure A-7

UNCONVENTIONAL
SIGNAL
PROCESSING
SBIR

The Spectrogram Underestimates the Slope of a Chirped Resonator

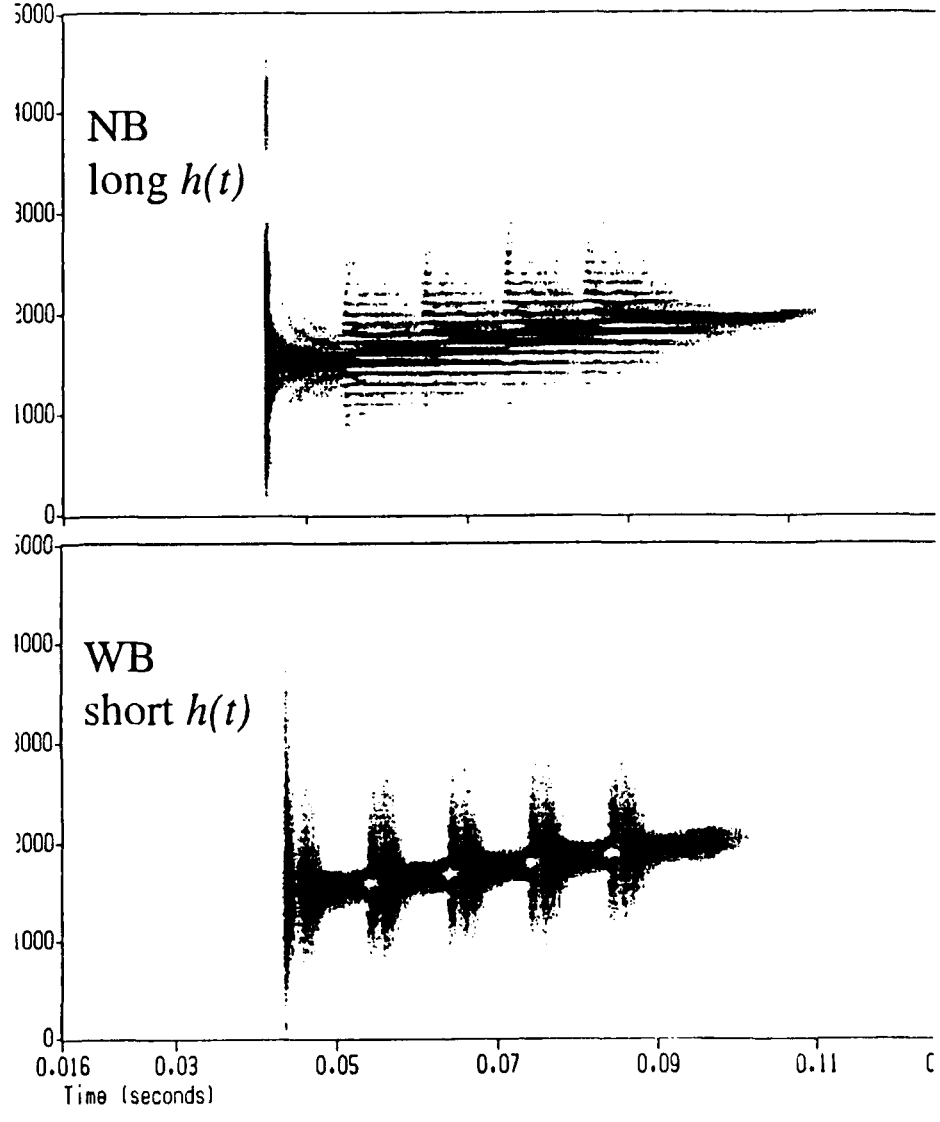

LE85.DRW

BLANK PAGE

Figure A-8

UNCONVENTIONAL
SIGNAL
PROCESSING
SBIR

Spectrogram Kernel

$h^*(t+\frac{\tau}{2})\ h\ (t-\frac{\tau}{2})$ in the (t,τ) Plane

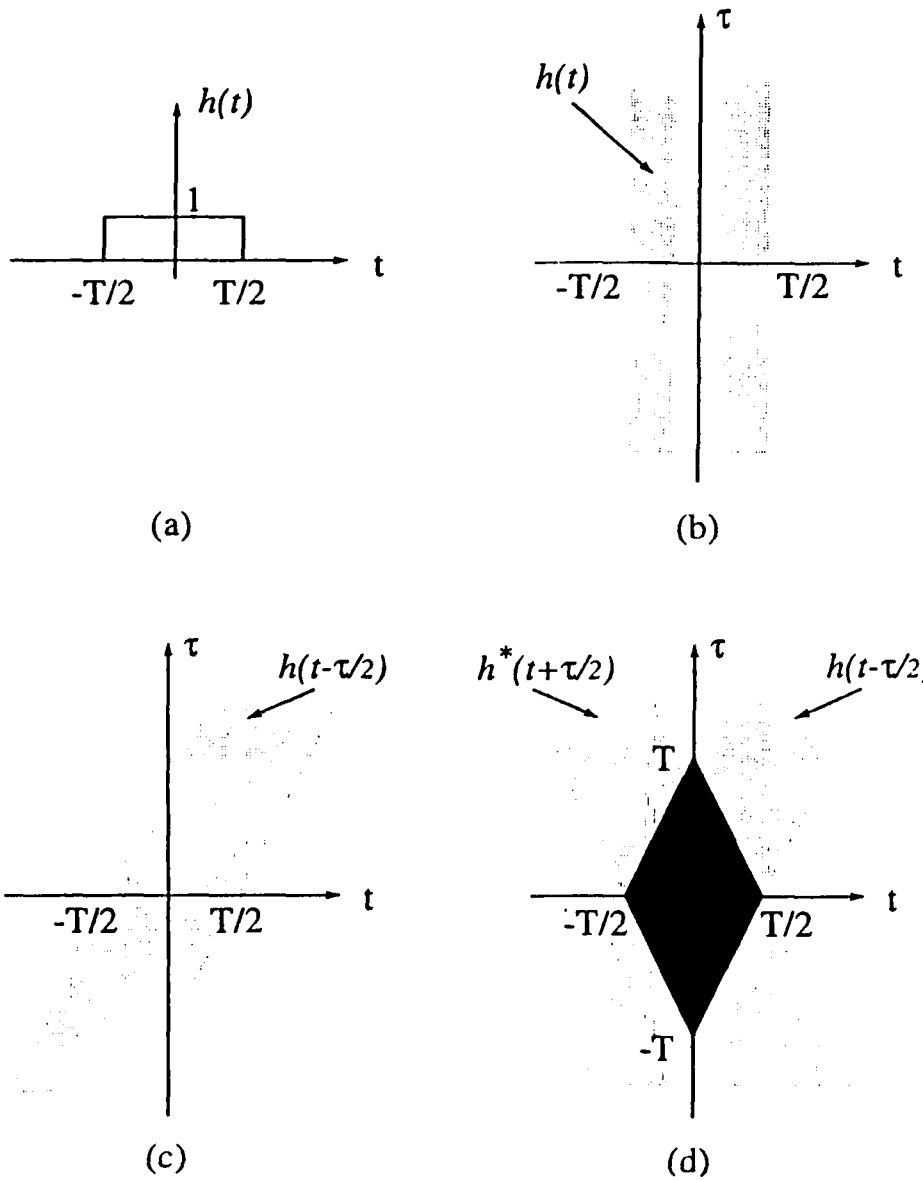

LES7.DRW

BLANK PAGE

Figure A-9

Other Kernel Choices

1. Wigner-Ville

$$\phi_w(t,\tau) = g(\tau)\,\delta(t)$$

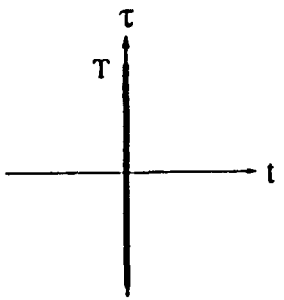

2. Cone Kernel [Zhao, Atlas & Marks]

$$\phi_{ck}(t,\tau) = g(\tau)\,rect\left(\frac{t}{\tau}\right)$$

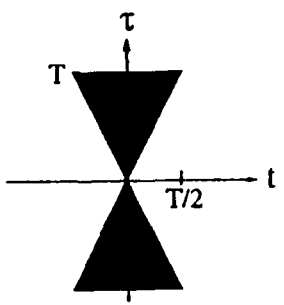

BLANK PAGE

UNCONVENTIONAL
SIGNAL
PROCESSING
SBIR

Figure A-10

Comparison of Five Time-Frequency Representations

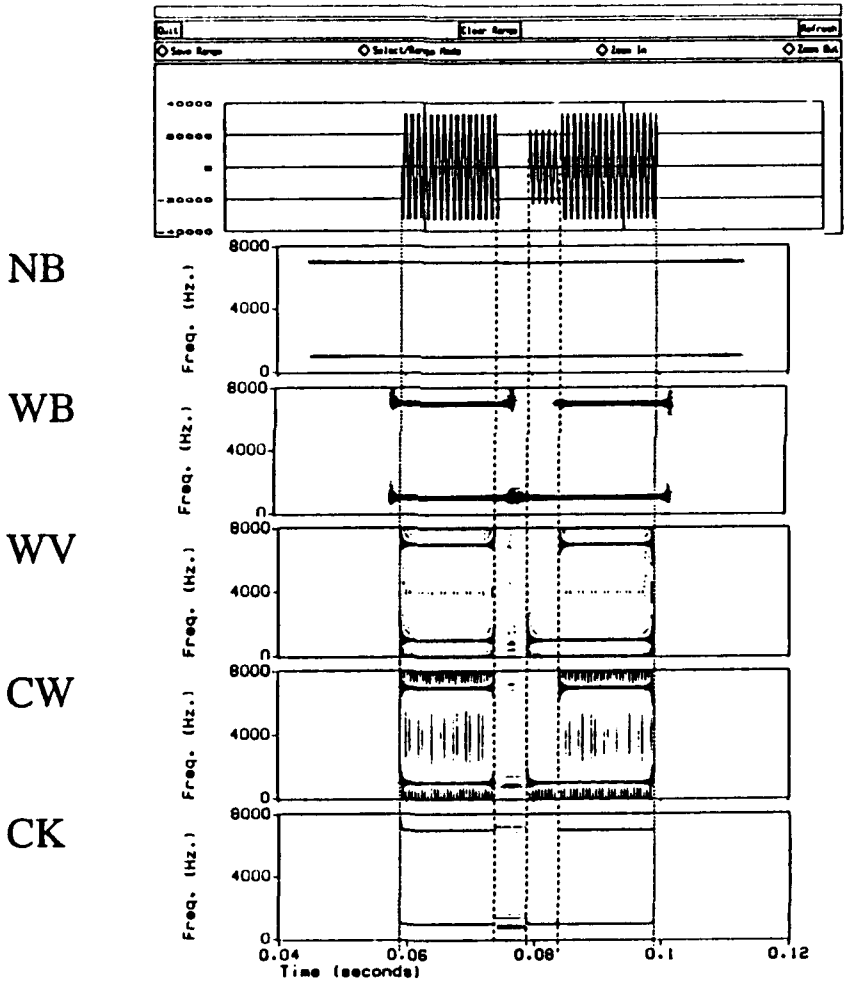

LES16.DRW

BLANK PAGE

UNCONVENTIONAL
SIGNAL
PROCESSING
SBIR

Figure A-11

Comparison on a Non-Stationary Tone

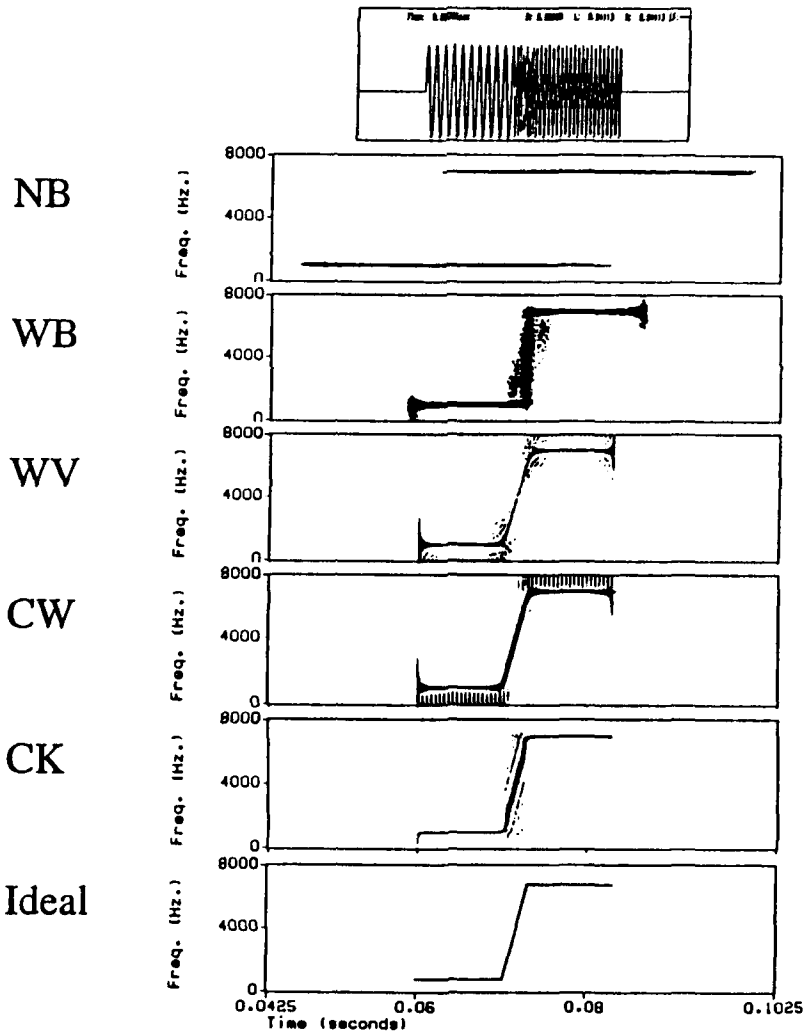

LEB17.DRW

BLANK PAGE

Table A-1

Summary of Properties

Table 1: Properties of Four Bilinear TFRs and the MCE-TFD

TFR	Non-negative	Marginals	Time Support	Frequency Support	Artifact Suppression
spectro-gram	YES	NO	NB/WB trade-off	NB/WB trade-off	GOOD
Wigner	NO	YES	WEAK	WEAK	SUCKS
Choi-Williams	NO	YES	VARIABLE	VARIABLE	VARIABLE
cone-kernel	NO	NO	WEAK	STRONG	GOOD

PERFORMANCE CHARACTERISTICS

Time & Frequency Resolution:

- Cone-kernel best for signals more complicated than single tones in quiet.

Artifact Suppression:

- Cone-kernel and spectrogram markedly better than other techniques.

Tracking Accuracy of Chirps:

- Cone-kernel best for signals more complicated than single tones in quiet.

BLANK PAGE

UNCONVENTIONAL
SIGNAL
PROCESSING
SBIR

Figure A-12

Single Whale Feeding Click With Single Screw in Background

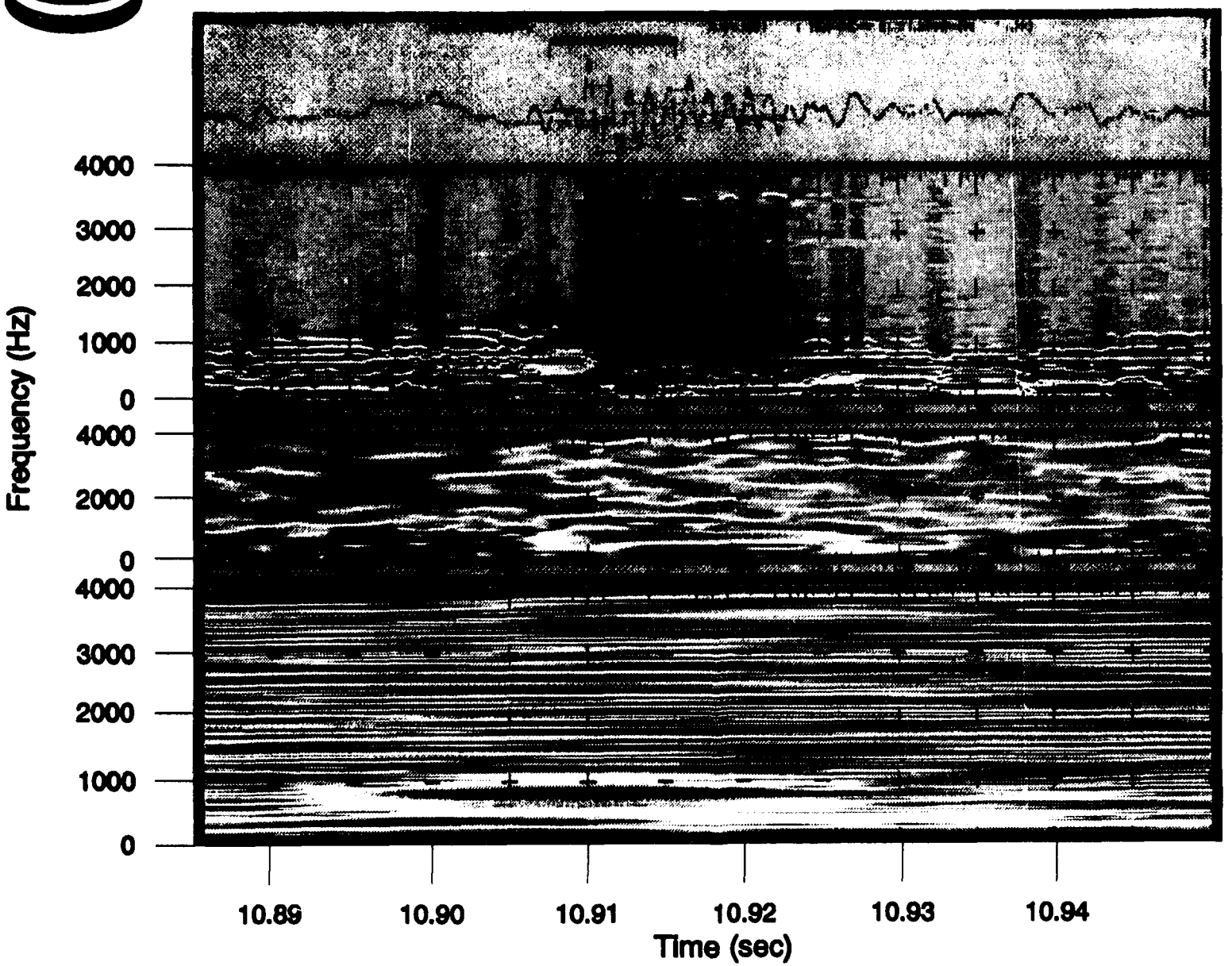

CLICK.DRW

UNCONVENTIONAL
SIGNAL
PROCESSING
SBIR

Figure A-13

Single Whale Call With Single Screw in Background

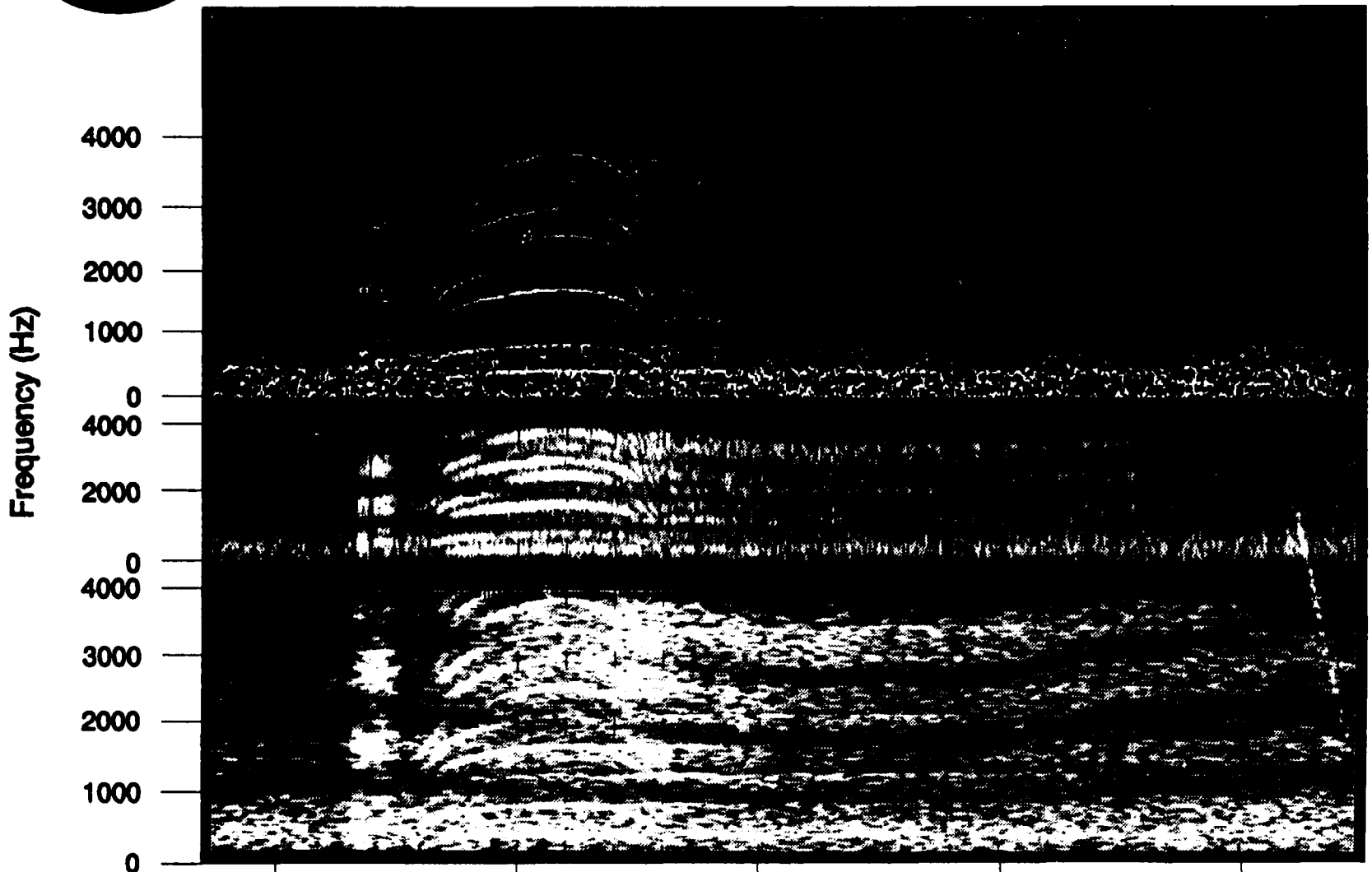

FEED1.DRW

UNCONVENTIONAL
SIGNAL
PROCESSING
SBIR

Figure A-14

Distant Diesel and Prop Noise in a Quiet Background

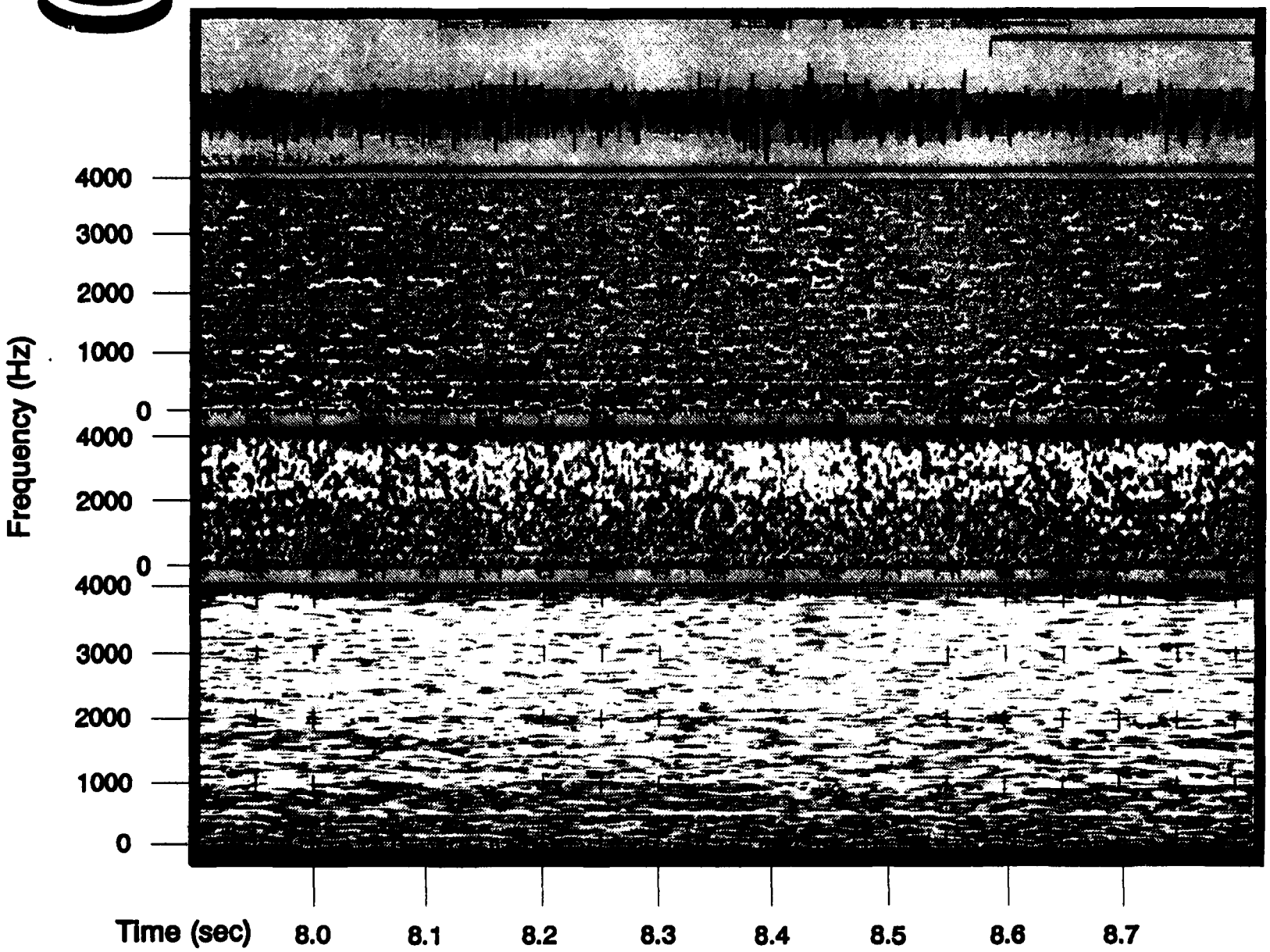

DPD.DRW

UNCONVENTIONAL
SIGNAL
PROCESSING
SBIR

Figure A-15

Close Diesel Engine with Hub Noise in Quiet Background

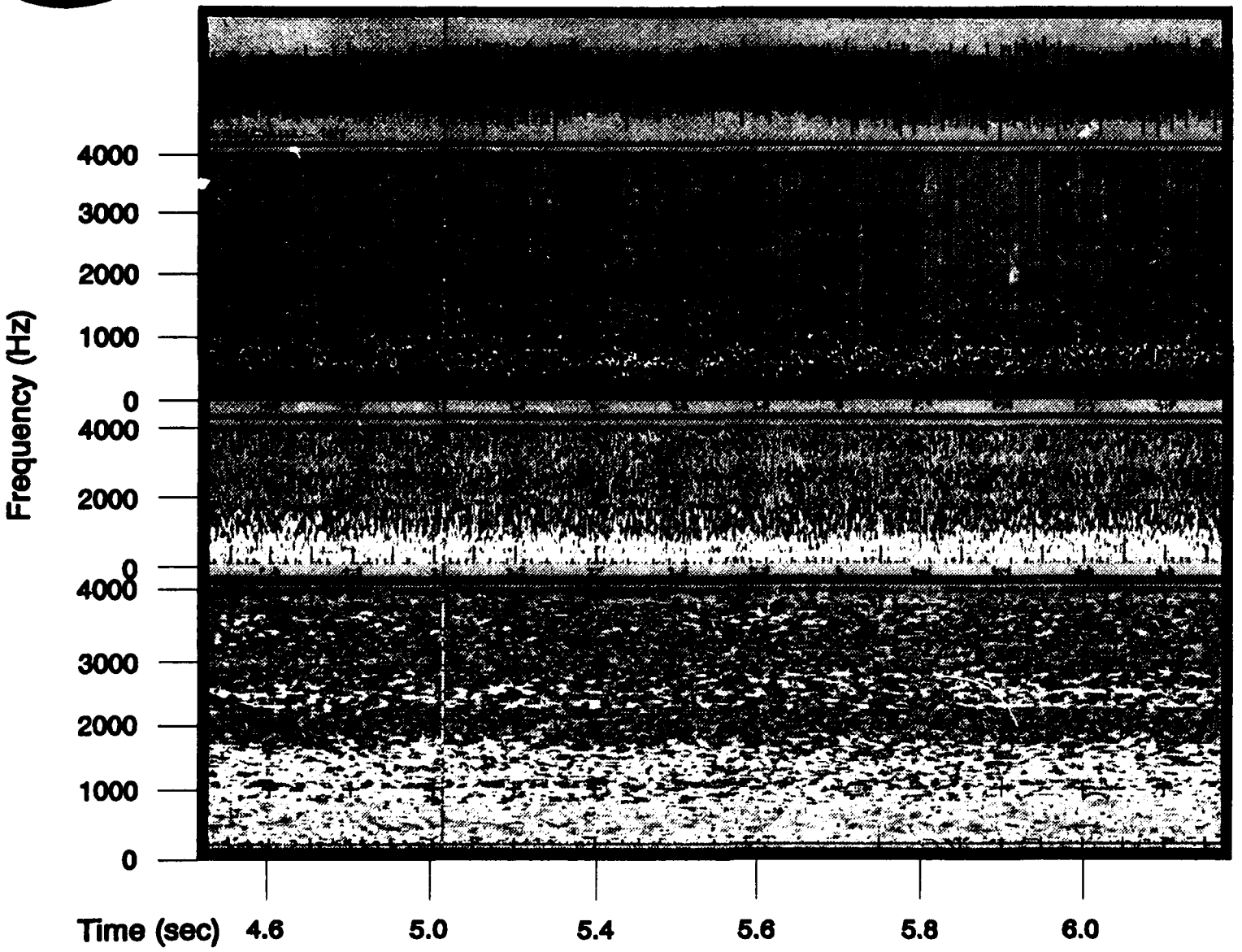

DIESEL_DRW

UNCONVENTIONAL
SIGNAL
PROCESSING
SBIR

Figure A-16

Detail of Close Diesel Engine with Hub Noise in Quiet Background

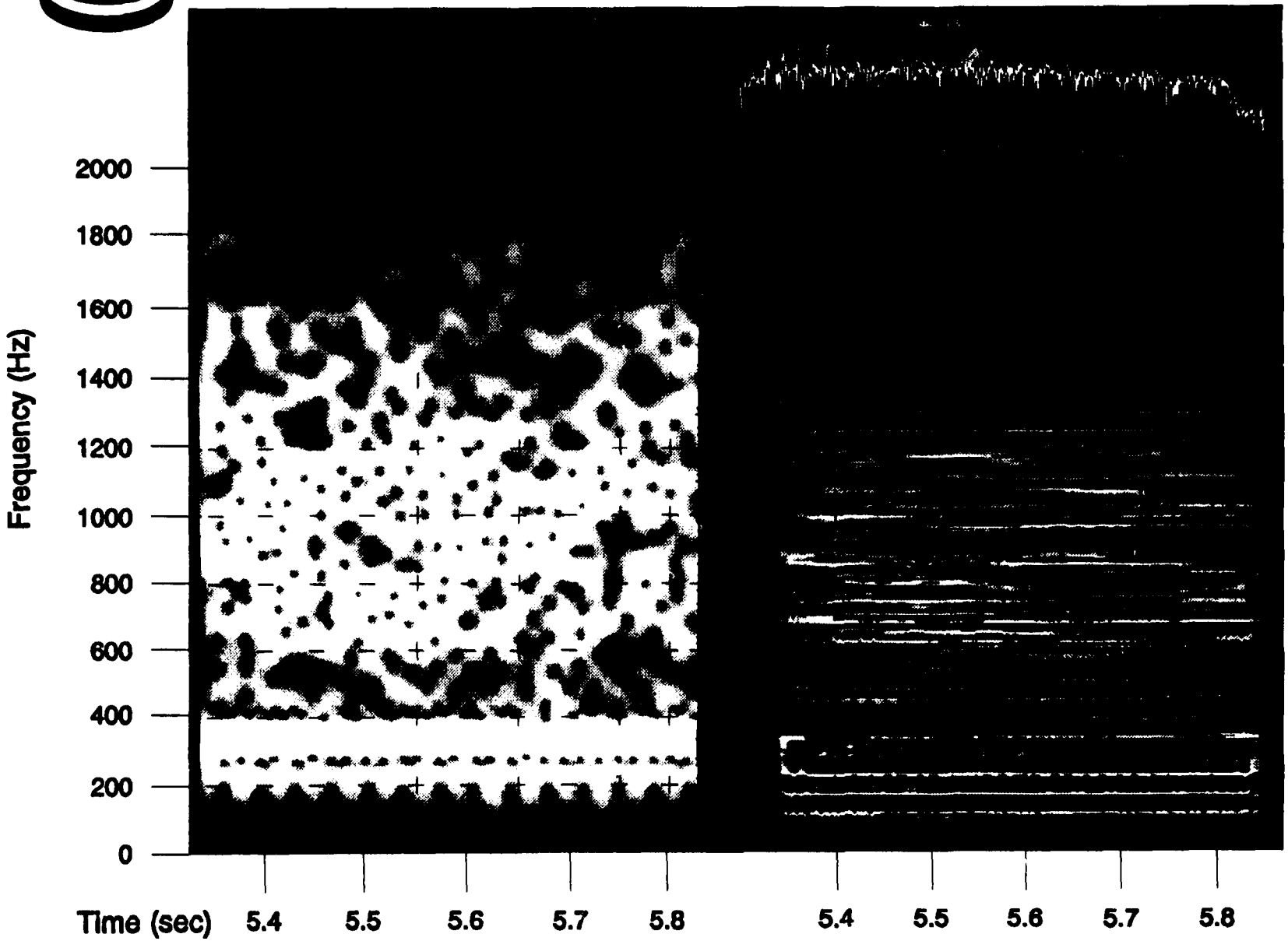

UNCONVENTIONAL
SIGNAL
PROCESSING
SBIR

Figure A-17

Single Whale Call and Screw in Synthetic Background Noise

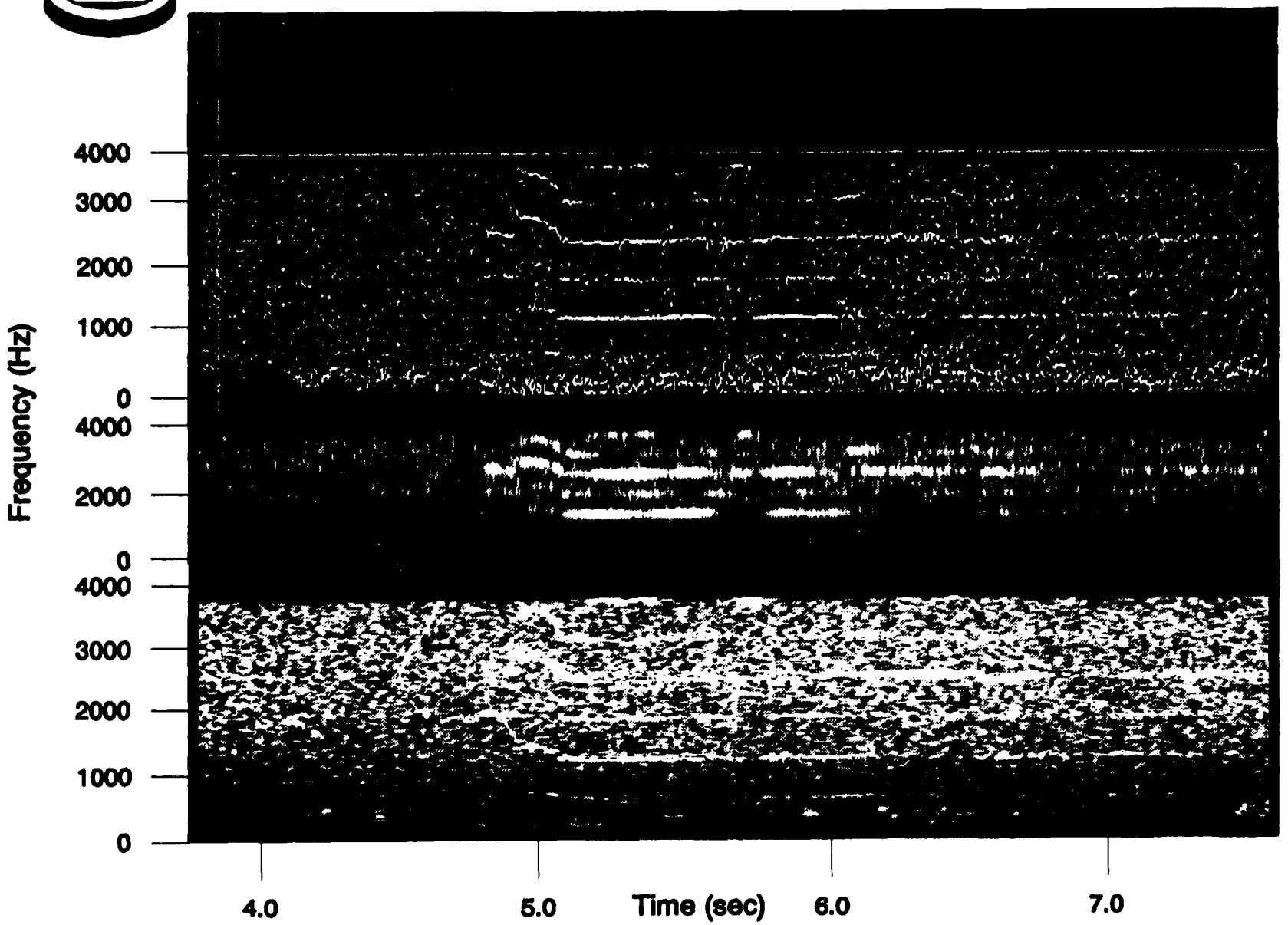

WHAPROP.DRW

UNCONVENTIONAL
SIGNAL
PROCESSING
SBIR

Figure A-18

Comparison On Simulated Active Sonar Signal

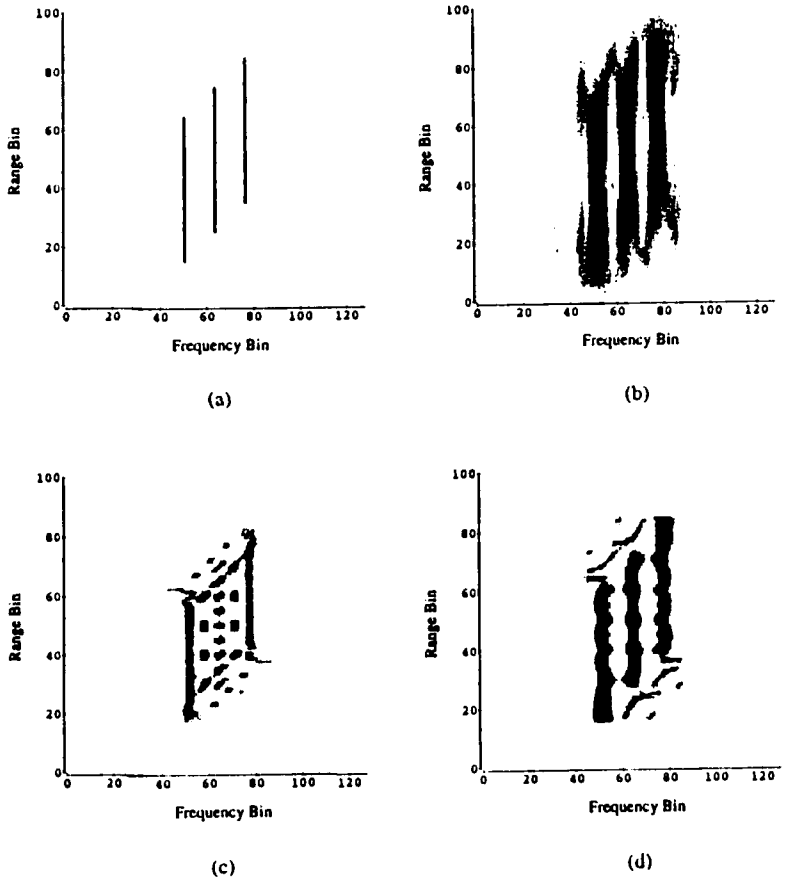

Density plots of simulated three-pulse return signal: (a) Ideal time-frequency plot, (b) Conventional cross-ambiguity function, (c) WVD, (d) new *Cone Kernel* technique

LES21.DRW

BLANK PAGE

Figure A-19

UNCONVENTIONAL
SIGNAL
PROCESSING
SBIR

Simulated Active Sonar Signal With 0 dB Signal-to-Noise Ratio

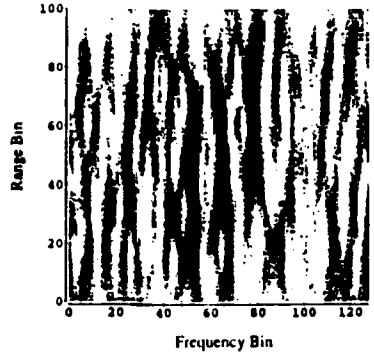

(a)

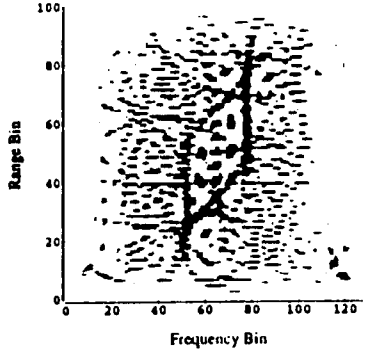

(b)

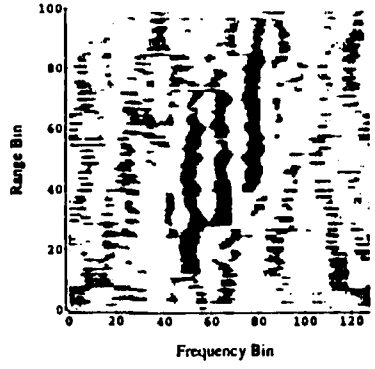

(c)

Density plots of simulated three-pulse return signal in additive white Gaussian noise, peak signal amplitude = noise standard deviation: (a) Conventional cross-ambiguity function, (b) WVD, (c) new *Cone Kernel* technique

LES22.DRW

BLANK PAGE

Figure A-20

The CK-TFR Process is Tractable - Fast Algorithms for its Discrete Implementation Exist

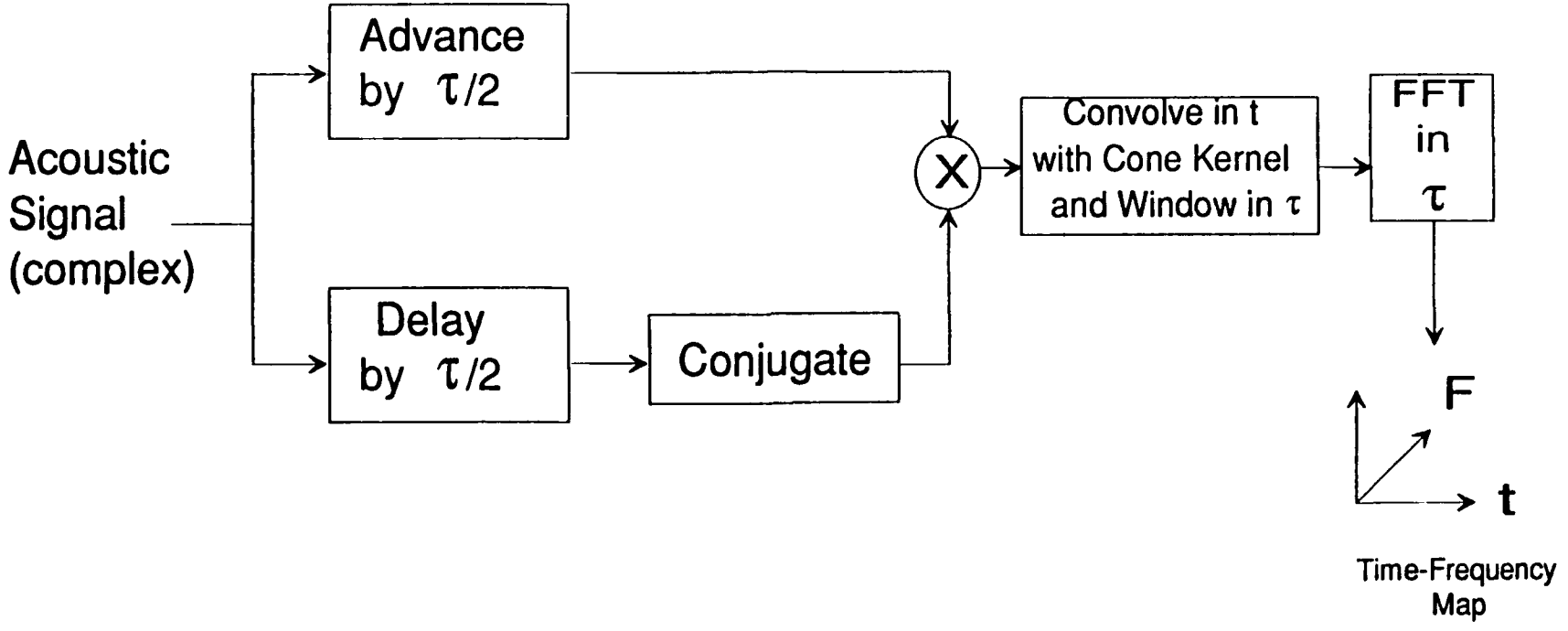

VG17.DRW

BLANK PAGE